ISTITUTO NAZIONALE DI FISICA NUCLEARE

Preventivo per l'anno ***2004***

Codice	Esperimento	Gruppo
	MAGO	2
Rapp. Naz.: Gianluca Gemme		

Rappresentante nazionale: Gianluca Gemme

Struttura di appartenenza: GE

Posizione nell'I.N.F.N.:

PROGRAMMA DI RICERCA

A) INFORMAZIONI GENERALI

Linea di ricerca	Ricerca di onde gravitazionali
Laboratorio ove si raccolgono i dati	INFN Genova
Sigla dello esperimento assegnata dal laboratorio	
Acceleratore usato	
Fascio (sigla e caratteristiche)	
Processo fisico studiato	Onde gravitazionali ad alta frequenza (4−10 kHz)
Apparato strumentale utilizzato	Cavità superconduttrici a radiofrequenza
Sezioni partecipanti all'esperimento	Genova, Napoli (Gr.Coll. Salerno)
Istituzioni esterne all'Ente partecipante	
Durata esperimento	Quattro anni (2004−2007)

B) SCALA DEI TEMPI : piano di svolgimento

PERIODO	ATTIVITA' PREVISTA
2004	a) Studio del refrigeratore ad elio superfluido sottoraffreddato; test di componenti critici b) Studio del sistema di sospensioni meccaniche; costruzione di prototipi c) Sviluppo test−bed e test di LNA (GaAs e InP) d) Modelli di sorgenti e analisi dati
2005	a) Progetto esecutivo del refrigeratore b) Test di prototipi e progetto esecutivo delle sospensioni c) Test componenti elettronici passivi a bassa temperatura d) Modelli di sorgenti e analisi dati
2006	a) Costruzione criostato b) Completamento test elettronica c) Modelli di sorgenti ed analisi dati
2007	Integrazione del sistema

ISTITUTO NAZIONALE DI FISICA NUCLEARE

Preventivo per l'anno **2004**

Codice	Esperimento	Gruppo
	MAGO	2
Resp. loc.: Innocenzo Pinto		

Struttura
SA

PREVENTIVO LOCALE DI SPESA PER L'ANNO 2004

In KEuro

VOCI DI SPESA		DESCRIZIONE DELLA SPESA	IMPORTI Parziali	SJ	Totale Compet.	SJ	A cura della Comm.ne Scientifica Nazionale
Viaggi e missioni	Interno	Missioni a Genova, Pisa e Legnaro	9.0	6.0	15.0	6.0	
	Estero	Missioni al Cern Partecipazioni a conferenze internazionali (MTT, GR, MG, GWDAW)	15.0	5.0	20.0	5.0	
Materiale Consumo					0.0	0.0	
Trasp. e facch.					0.0	0.0	
Spese Calcolo		Consorzio / Ore CPU / Spazio Disco / Cassette / Altro			0.0	0.0	
Affitti e manutenz. apparecchiat.		SW APLAC (simulatore EM)	10.0		10.0	0.0	
Materiale inventariabile		Componentistica in guida; Quad−DSP PCI board (C6701)	20.0		20.0	0.0	
Costruzione Apparati					0.0	0.0	
			Totale		**65.0**	**11.0**	

Sono previsti interventi e/o impiantistica che ricadono sotto la disciplina della legge Merloni ? ☐

Breve descrizione dell'intervento:

Mod EC./EN. 2 (a cura del responsabile locale)

ISTITUTO NAZIONALE DI FISICA NUCLEARE

Preventivo per l'anno ***2004***

Struttura
SA

Codice	Esperimento	Gruppo
	MAGO	2
Resp. loc.: Innocenzo Pinto		

ALLEGATO MODELLO EC2

Le richieste finanziarie fanno riferimento a:
i) spese di missione inerenti alla collaborazione tra gruppi proponenti;
ii) partecipazione a conferenze internazionali su temi specifici del progetto;
iii) acquisto di SW per la simulazione di circuiti a microonde (licenze);
iv) acquisto di componentistica a microonde

La base di partenza dell'Unita' e' descritta nei files allegati:

SA_MAGO all 1 (pubblicazioni recenti in materia di rivelazione di onde gravitazionali)
SA_MAGO all 2 (pubblicazioni recenti in materia di componenti e circuiti a microonde)
SA_MAGO all 3 (principali dotazioni strumentali per la simulazione ed il testing di componenti e circuiti a microonde).

ISTITUTO NAZIONALE DI FISICA NUCLEARE

Preventivo per l'anno ***2004***

Struttura
SA

Codice	Esperimento	Gruppo
	MAGO	2
Resp. loc.: Innocenzo Pinto		

ALLEGATO MODELLO EC2

Pubblicazioni recenti dell'Unita' (selezione)
in materia di componenti e circuiti a microonde

G. Castaldi, V. Fiumara, I.M. Pinto, "A Dual-Band Chebishev Impedance Transformer", *Microwave Opt. Tech. Lett.*, October 2003, in print.

G. Chiadini, V. Fiumara, I.M. Pinto, A. Scaglione, "Self Scaling Properties of the Reflection Coefficient of Cantor Pre-Fractal Multilayers", *Microwave Opt. Tech. Lett.*, 37, 339, 2003.

V. Galdi and L.B. Felsen, "Two-dimensional Pulsed Propagation from Extended Aperture Field Distributions through a Planar Dielectric Layer via Quasi-ray Gaussian Beams," *IEEE Trans. Antennas and Propagat.*, 51, 1549, 2003.

V. Galdi, L.B. Felsen, and D.A. Castañon, "Time-domain Radiation from Large Two-dimensional Apertures via Narrow-waisted Gaussian Beams," *IEEE Trans. Antennas and Propagat.*, 51, 1, 78, 2003.

V. Galdi, H. Feng, D.A. Castañon, W.C. Karl, and L.B. Felsen, "Multifrequency Subsurface Sensing in the Presence of a Moderately Rough Air-soil Interface Via Quasi-Ray Gaussian Beams," *Radio Science*, vol. 37, No. 6 (Special Issue, invited paper), 2002.

V. Galdi, L.B. Felsen, and D.A. Castañon, "Quasi-ray Gaussian Beam Algorithm for Time-harmonic Two-dimensional Scattering by Moderately Rough Interfaces," *IEEE Trans. Antennas and Propagat.*, 49, 1305, 2001.

V. Galdi, L.B. Felsen, I.M. Pinto, "Applications of Path Integrals to Electromagnetics: a Critical Survey", *Atti della Fondazione Giorgio Ronchi*, Sept. 2001.

V. Galdi, L.B. Felsen and L.Castañon, "Narrow-waisted Gaussian Beam Discretization for Short-Pulse Radiation from One-Dimensional Large Apertures", *IEEE Trans. Antennas Propagat.*, 49, 1322, 2001.

V. Galdi and I.M. Pinto, "Derivation of Higher-Order Impedance Boundary Conditions for Stratified Coatings Composed of Inhomogeneous-Dielectric and Homogeneous-Bianisotropic Layers", *Radio Science*, 35, 287, 2000.

V. Galdi, I.M. Pinto, "A Simple Algorithm for Accurate Location of Leaky-wave Poles for Grounded Inhomogeneous Dielectric Slabs", *Microwave Opt. Technol. Lett.*, 24, 135, 2000.

V. Galdi, V. Fiumara, V. Pierro, I.M. Pinto, "Analytical Approximations for Fundamental Mode Field and Dispersion Equation of Planar Waveguides through Stevenson-Pade’ Approach", *Microwave Opt. Technol. Lett.*, 27, 158, 2000.

G. Castaldi, V. Pierro, and I.M. Pinto, "Efficient Faulty Element Diagnostics of Large Antenna Arrays by Discrete Mean-Field Neural Nets", *Progress in Electromagnetics Research* (PIER), J.A. Kong, Ed., 25, 53, 2000.

Pubblicazioni recenti dell'Unita' (selezione)
in materia di rivelazione di onde gravitazionali

R.P. Croce, Th. Demma, M. Longo, S. Marano, V. Matta, V. Pierro, I.M. Pinto, "Gravitational Wave Chirp Search: no Signal Cumulative Distribution of the Maximum Likelihood Detection Statistic", *Class. Quantum Grav.*, 20,1, 2003.

V. Pierro, I. M. Pinto, A.D. Spallicci, "Computation of Hyper^n Geometric Functions for Gravitationally Radiating Binary Stars", *Mon. Not. Royal Astron. Soc.*, 334, 855, 2002.

V. Pierro, I. M. Pinto, A.D. Spallicci, E. Laserra, F. Recano, "Fast and Accurate Computational Tools for Gravitational Waveforms from Binary Stars with any Orbital Eccentricity", *Mon. Not. Royal Astron. Soc.*, 325, 358, 2001.

R.P.Croce, Th. Demma, V. Pierro, I. M. Pinto, "More on the Tanaka-Tagoshi Parametrization of post-1PN Spin-Free Gravitational Wave Chirps: Equispaced and Cardinal Interpolated Lattices", *Physical Review*, D64, 087101, 2001.

R.P.Croce, Th. Demma, V. Pierro, I. M. Pinto, "Tanaka-Tagoshi Parametrization of post-first-post-Newtonian Spin-Free Gravitational Wave Chirps: Equispaced and Cardinal Interpolated Lattices for First Generation Interferometric Antennas", *Physical Review*, D64, 042005, 2001.

R.P.Croce, Th. Demma, V. Pierro, I. M. Pinto, B. Churches, B.S. Sathyaprakash, "Gravitational Wave Chirp Search: Economization of Post Newtonian Matched Filter Bank via Cardinal Interpolation", *Physical Review*, D62, 12101(R), 2000.

R.P.Croce, Th. Demma, V. Pierro, I. M. Pinto, F. Postiglione, "Nearly Minimum Redundant Correlator Interpolation Formula for Gravitational Wave Chirp Detection", *Physical Review*, D62, 124020, 2000.

R.P. Croce, Th. Demma, V. Pierro**,** I.M. Pinto, F. Postiglione, "A Minimum Redundant Cardinal Interpolated Correlator for Binary Chirp Detection", in *Gravitational Wave Detection, II*, S. Kawamura and N. Mio Eds., Universal Acad. Press, Tokyo, 2000, ISBN 4-946443-56-8, p. 251. (PDF)

Principali dotazioni strumentali dell'Unita'
Per la simulazione ed il testing di componenti e circuiti a microonde

- Analizzatore di reti vettoriale fino a 50GHz Agilent 85107B (bundle);
- Oscilloscopio TDR a microonde Hewlett-Packard 54124T+54121;
- NF-FF Scanner ORBIT-FR AL 4952-7-7-V-CS (6 assi) con controllore (AL4706-3A + 4146-2);
- Ricevitore a Microonde fino a 50GHz HP8530A/010 + HP8511B;

- Cluster di 16 CPU (PIII/1000-133, 1GBRAM, 120GBHD per nodo) in ambiente LINUX/MOSIX.

- GRID-MATHEMATICA@; QFDTD90; etc.

ISTITUTO NAZIONALE DI FISICA NUCLEARE

Preventivo per l'anno ***2004***

Codice	Esperimento	Gruppo
	MAGO	2
Rapp. Naz.: Gianluca Gemme		

PREVENTIVO GLOBALE DI SPESA PER L'ANNO 2004

In KEuro

Struttura	A CARICO DELL' I.N.F.N.																		A carico di altri Enti
	Miss. interno	di cui **SJ**	Miss. estero.	di cui **SJ**	Materiale di cons.	di cui **SJ**	Trasp. e Facch.	di cui **SJ**	Spese Calc.	di cui **SJ**	Affitti e Manut. Appar.	di cui **SJ**	Mater. inventar.	di cui **SJ**	Costr. appar.	di cui **SJ**	TOTALE Compet.	di cui **SJ**	
GE	20,0		39,0		25,0						7,5		51,5		28,0		171,0		0,0
SA	15,0	6,0	20,0	5,0							10,0		20,0				65,0	11,0	0,0
TOTALI	**35,0**	**6,0**	**59,0**	**5,0**	**25,0**						**17,5**		**71,5**		**28,0**		**236,0**	**11,0**	

NB. La colonna A carico di altri enti deve essere compilata obbligatoriamente

Note:

Mod EC./EN. 4

(a cura del responsabile nazionale)

Nuovo esperimento	Gruppo
MAGO	2

PROPOSTA DI NUOVO ESPERIMENTO

In a series of papers, since 1978, it has been studied how the energy transfer induced by the gravitational wave between two levels of an electromagnetic resonator, whose frequencies f1 and f2 are both much larger than the characteristic angular frequency F of the g.w., could be used to detect gravitational waves. The energy transfer is maximum when the resonance condition f2−f1 = F is satisfied. This is an example of a frequency converter, i.e. a nonlinear device in which energy is transferred from a reference frequency to a different frequency by an external pump signal.
In the scheme suggested by Bernard et al. the two levels are obtained by coupling two identical high frequency cavities. Each resonant mode of the individual cavity is then split in two modes of the coupled resonator with different spatial field distribution. In the following we shall call them the symmetric and the antisymmetric mode. The frequency difference of the two modes (the detection frequency) is determined by the coupling, and can be tuned by a careful resonator design. An important feature of this device is that the detection frequency does not depend on its mechanical properties (dimensions, weight and mechanical modes resonant frequencies). Of course, the detector can be tuned so that the mode splitting equals the frequency of a mechanical resonant mode. The sensitivity in this and other experimental situations will be discussed in the following. Since the detector sensitivity is proportional to the electromagnetic quality factor, Q, of the resonator, superconducting cavities should be used for maximum sensitivity.

An RDeffort, funded by the 5th Scientific Committee of INFN, started in 1998 and will be completed at the end of 2003 (PACO, 1998−2000; PACO−2, 2001−2003). Its main objective is the development of a tunable detector of small harmonic displacements based on two coupled superconducting cavities. Several cavity prototypes (both in copper and in niobium) were built and tested, and finally a design based on two spherical cells was chosen and realized. The detection frequency, i.e. the frequency difference between the symmetric and antisymmetric modes, was chosen to be: f2−f1 ~ 10 kHz (the frequency of the modes being f1,f2 ~ 2 GHz. An electromagnetic quality factor Q > 10^(10) was measured on a prototype with fixed coupling.
The tuning system was also carefully studied. The coupling strength, and thus the tuning range, is determined by the diameter of the coupling tube and by the distance between the two sperical cells. A central elliptical cell, which can easily be streched and squeezed, was found to provide a tuning range of several kHz (4−20 kHz in the final design). A prototype with the central elliptical cell was built and is now being tested. A second tunable cavity (two spherical cells and the central elliptical cell) is being commissioned, and will be ready by the middle of 2004.
The system was also mechanically characterized, and the mechanical resonant modes in the frequency range of interest were identified. In particular the quadrupolar mode of the sphere was found to be at 4 kHz, in good agreement with finite elements calculations.
The detection electronics was designed. Its main task is to provide the rejection of the symmetric mode component at the detection frequency. A rejection better than 150 dB was obtained in the final system.
Starting from the results obtained in the last six years, we are now planning to design and realize an experiment for the detection of gravitational waves in the 4−10 kHz frequency range. Our main task is the design and construction of the refrigerator and of the cryostat (including the suspension system), which houses the coupled cavities. The refrigerator must provide the cryogenic power needed to keep the superconductiong cavities at T ~ 1.8 K (approx. 10 Watts) without introducing an excess noise from the external environment. A design based on the use of subcooled superfluid helium is being invesigated.
The expected time−scale is four years (2004−2007).

MAGO

Microwave Apparatus for Gravitational Waves Observation

Research Proposal to INFN

(July 2003)

R. Ballantini[a], Ph. Bernard[b], S. Calatroni[b], E. Chiaveri[b], A. Chincarini[a], R.P. Croce[c], S. Cuneo[a], V. Galdi[c], G. Gemme[a,1], R. Losito[b], R. Parodi[a], E. Picasso[d], V. Pierro[c], I.M. Pinto[c], A. Podestà[a], R. Vaccarone[a]

[a] *INFN and Università degli Studi di Genova, Genova, Italy*
[b] *CERN, Geneva, Switzerland*
[c] *INFN, Napoli, and Università degli Studi del Sannio, Benevento, Italy*
[d] *INFN and Scuola Normale Superiore, Pisa, Italy*

[1] Spokeperson

Contents

1 Experiment overview

In the last decades, several laboratories all around the world have promoted an intense effort devoted to the direct detection of gravitational waves. The detectors, both those in operation and those being developed, belong to two conceptually different families, massive elastic solids (cylinders or spheres) [1] and Michelson interferometers [2]. Both types of detectors are based on the mechanical coupling between the gravitational wave and a test mass, and in both types the electromagnetic field is used as motion transducer.

In a series of papers, since 1978, it has been studied how the energy transfer induced by the gravitational wave between two levels of an electromagnetic resonator, whose frequencies ω_1 and ω_2 are both much larger than the characteristic angular frequency Ω of the g.w., could be used to detect gravitational waves [3, 4]. The energy transfer is maximum when the resonance condition $|\omega_2 - \omega_1| = \Omega$ is satisfied. This is an example of a frequency converter, i.e. a nonlinear device in which energy is transferred from a reference frequency to a different frequency by an external pump signal.

In the scheme suggested by Bernard et al. the two levels are obtained by coupling two identical high frequency cavities [4]. Each resonant mode of the individual cavity is then split in two modes of the coupled resonator with different spatial field distribution. In the following we shall call them the *symmetric* and the *antisymmetric* mode. The frequency difference of the two modes (the detection frequency) is determined by the coupling, and can be tuned by a careful resonator design. An important feature of this device is that the detection frequency does not depend on its mechanical properties (dimensions, weight and mechanical modes resonant frequencies), though, of course, the detector *can* be tuned so that the mode splitting equals the frequency of a mechanical resonant mode. The sensitivity in this and other experimental situations will be discussed in the following. Since the detector sensitivity is proportional to the electromagnetic quality factor, $\mathcal{Q}$, of the resonator, superconducting cavities should be used for maximum sensitivity.

An R&D effort, funded by the 5^{th} Scientific Committee of INFN, started in 1998 and will be completed at the end of 2003 (PACO, 1998–2000; PACO–2, 2001–2003) [5, 6]. Its main objective is the development of a *tunable* detector of small harmonic displacements based on two coupled superconducting cavities. Several cavity prototypes (both in copper and in niobium) were built and tested, and finally a design based on two spherical cells was chosen and realized (Fig. 1). The detection frequency, i.e. the frequency *difference* between the symmetric and antisymmetric modes, was chosen to be: $\omega_2 - \omega_1 \approx 10$ kHz (the frequency of the modes being $\omega_{1,2} \approx 2$ GHz). An electromagnetic quality factor $\mathcal{Q} > 10^{10}$ was measured on a prototype with fixed coupling (Fig. 2).

The tuning system was also carefully studied. The coupling strength, and thus the tuning range, is determined by the diameter of the coupling tube and by the distance between the two sperical cells. A central elliptical cell, which can easily be streched and squeezed, was found to provide a tuning range of several kHz (4–20 kHz in the final design). A prototype with the central elliptical cell was built and is now being tested (Fig. 3). A second tunable cavity (two spherical cells and the central elliptical cell) is being commissioned, and will be ready by the middle of 2004.

The system was also mechanically characterized, and the mechanical reso-

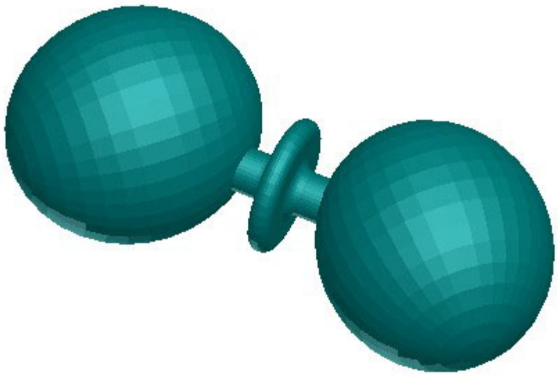

Figure 1: Artistic view of the coupled spherical cavities with the central tuning cell

Figure 2: Niobium spherical cavities (fixed coupling)

nant modes in the frequency range of interest were identified. In particular the quadrupolar mode of the sphere was found to be at 4 kHz, in good agreement with finite elements calculations.

The detection electronics was designed. Its main task is to provide the rejection of the symmetric mode component at the detection frequency. A rejection better than 150 dB was obtained in the final system.

Starting from the results obtained in the last six years, we are now planning to design and realize an experiment for the detection of gravitational waves in the 4–10 kHz frequency range. Our main task is the design and construction of the refrigerator and of the cryostat (including the suspension system), which houses the coupled cavities. The refrigerator must provide the cryogenic power needed to keep the superconductiong cavities at $T \approx 1.8$ K (approx. 10 Watts) without introducing an excess noise from the external environment. A design based on the use of subcooled superfluid helium is being invesigated. The expected time-scale is four years (2004–2007).

In the following a detailed description of the various issues aforementioned will be given. Expected system sensitivity will also be discussed.

Figure 3: Niobium spherical cavities (variable coupling)

2 Physics motivation

The spectrum of gravitational waves of cosmic origin targeted by currently operating or planned detectors spans roughly [2] from 10^{-4} to 10^{4} Hz.

The $f \leq 10^{-1}$ Hz region of the GW spectrum, including galactic binaries [7], (super)massive BH binary inspirals and mergers [8], compact object inspirals and captures by massive BHs [9], will be thoroughly explored by LISA [10], which might be hopefully flown by year 2015. Ground based interferometers and acoustic detectors (bars and spheres) will likewise co–operate in exploring the $f \geq 10^1 Hz$ region of the spectrum, including compact binary inspirals and mergers [11], supernovae and newborn black-hole ringings [12], fast-spinning non-axisymmetric neutron stars [13], and stochastic GW background [14].

The whole spectral range from $10^{-4} - 10^{4}$ Hz, however, is far from being covered with uniform sensitivity, as seen e.g. from Fig. 4, where the fiducial sensitivity curves of LISA and LIGO–II are shown side by side. Plans are being made for small–scale LISA–like space experiments (e.g., DECIGO, [15]) aimed at covering the frequency gap $10^{-1} - 10^{1}$ Hz between LISA and terrestrial detectors.

Several cryogenic/ultracryogenic acoustic (bar) detectors are also operational, including ALLEGRO [16], AURIGA [17], EXPLORER [18], NAUTILUS [19], and NIOBE [20]. They are tuned at $\sim 10^3$ Hz, with bandwidths of a few tens of Hz, and minimal noise PSDs of the order of 10^{-21} Hz$^{-1/2}$.

Intrinsic factors exist which limit the performance of both IFOs and acoustic detectors in the upper frequency decade ($f \gtrsim 10^3$ Hz) of the spectrum.

The high frequency performance of laser interferometers is limited by the $\propto f^2$ raise of the laser shot-noise floor. While it is possible to operate IFOs in a resonant (dual) light-recycled mode, for narrow-band increased-sensitivity operation (see Fig. 5), the pitch frequency should be kept below the suspension

[2] We leave out deliberately the ELF ($10^{-18} - 10^{-15}$ Hz) radiation resulting from inflation–enhanced primordial gravitational fluctuations, expected to show up in the polarization anisotropy of the cosmic microwave background (M. Kamionkowski, A. Jaffe, Int, J. Mod. Phys. A16, 116, 2001), the VLF ($10^{-7} - 10^{-9}$ Hz) radiation possibly resulting from extremely massive black-hole systems and early–universe processes (A.N. Lommen and D.C. Backer, Astrophys. J., 562, 297, 2001, astro-ph/0107470), exotic electromagnetic–to–gravitational wave conversion mechanisms, which might originate gravitational radiation in the VHF to SHF bands (Fang-Yu Li and Meng-Xi Tang, Int. J. Mod. Phys D11, 1049, 2002) and the relic gravitational radiation (B. Allen and R. Brustein, Phys. Rev. D55, 3260, 1997).

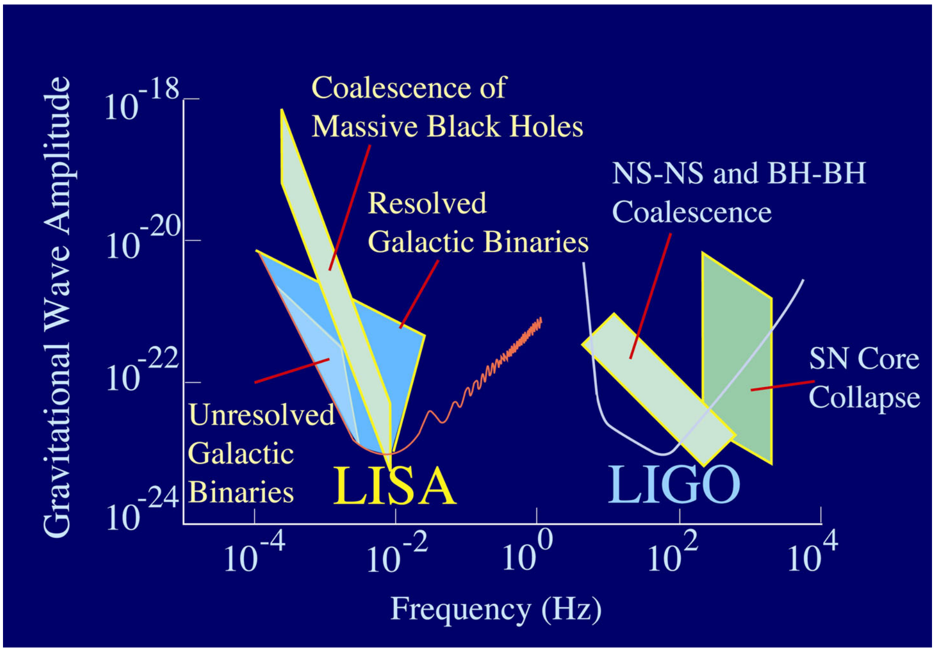

Figure 4: LISA–LIGO comparison

violin-modes [21], typically clustering near and above $\sim 5 \cdot 10^2$ Hz.

Increasing the resonant frequency of acoustic detectors (bars, spheres and TIGAs), on the other hand, requires decreasing their mass M. The high frequency performance of bars and spheres is accordingly limited by the $\propto M^{-1/2}$ dependance of the acoustic detectors' noise PSD.

The next generation of resonant detectors will be probably spheres or TIGAs (Truncated Icosohedral Gravitational Antennas, [22]) [3] The MINIGRAIL [23] spherical prototype[4] experiment under construction at Leiden University (NL), as well as its twins planned by the Rome group [24] and at São Paulo, Brazil [25], is a relatively small (CuAl (6%) alloy, $\emptyset$ 65cm, 1.15ton) spherical ultracryogenic (20mK) detector with a 230Hz bandwidth centered at 3250Hz, and a (quantum limited) strain sensitivity of $h \sim 4 \cdot 10^{-21}$. Spherical (or TIGA) detector might achieve comparable sensitivities up to $f \sim 4 \cdot 10^3$ Hz.

Summing up, the GW spectrum below $f \sim 10^3$ Hz might be adequately covered by ground-based and space-borne interferometers. The range between 10^3 Hz and $\sim 4 \cdot 10^3$ Hz could be sparsely covered by new-generation acoustic detectors. The high frequency part ($f \gtrsim 4 \cdot 10^3$ Hz) of the gravitational wave spectrum of cosmic origin is as yet completely uncovered. Within this band,

[3] Spheres and TIGAs share the nice feature of being inherently omnidirectional, and should allow to reconstruct the direction of arrival and polarization state of any detected gravitational wave, by suitably combining the outputs of transducers gauging the amplitudes of the five degenerate quadrupole sphere modes (C. Zhou and P.F. Michelson, Phys. Rev. D51, 2517, 1995).

[4] A cryogenic solid-CuAl sphere resonating at $\sim 10^3$ Hz would be ~ 4 m $\emptyset$ and weigh in excess of 100 tons. The related technological challenges could be alleviated by resorting to hollow geometries (J.A. Lobo, Class. Quantum Grav., 19, 2029, 2002).

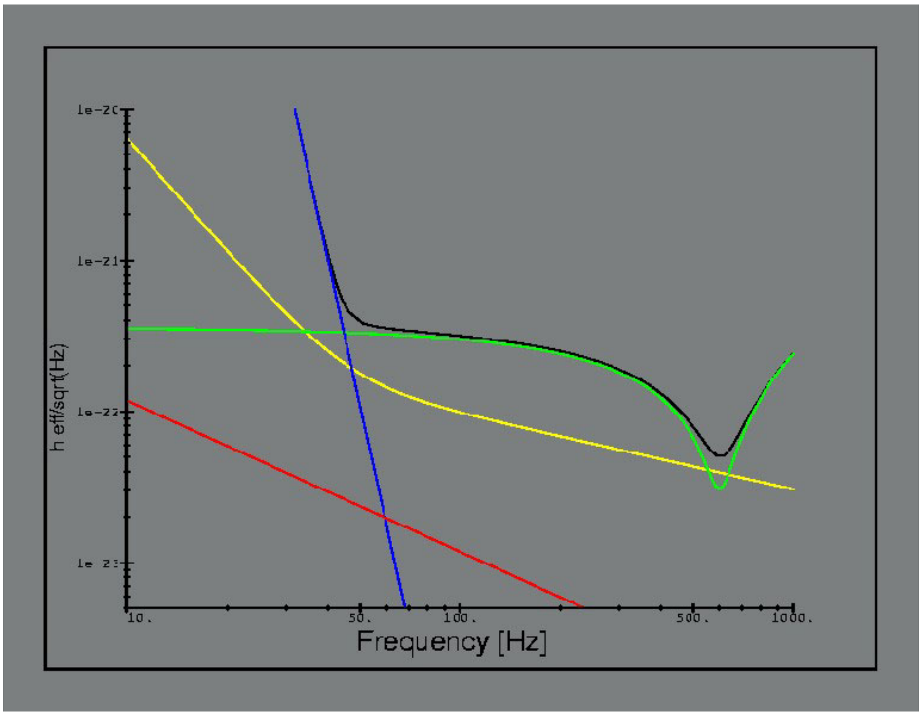

Figure 5: The narrowband response of GEO600. The picture shows the spectral densities of the amplitudes of apparent gravitational waves which give the same detector output as the various noise sources. (Black: overall noise; green: shot noise; blue: seismic noise; yellow: thermal noise; red: standard quantum limit. Courtesy of GEO600)

GW sources might well exist and be observed [5]. Indeed, the ultimate goal of gravitational-wave astronomy is the discovery of *new* physics. In this spirit, the very existence of gravitational wave sources of as yet unknown kind could not be excluded a-priori.

The above brings strong conceptual and practical motivations for the MAGO proposal. The MAGO design is easily scalable, and may be constructed to work at *any* chosen frequency in the range $10^3 - 10^4$ Hz, with uniform (narrowband) performance. On the other hand, the MAGO instrument appears to be comparatively cheap and lightweigth, thus allowing to build as many detectors as needed to ensure adequate covering of the high frequency ($f \gtrsim 4 \cdot 10^3$ Hz) GW spectrum. In view of their limited cost, MAGOs might also be nice candidates for many–detector networks, to achieve very low false alarm probabilities in coincidence operation. In addition MAGO–like detectors operating at $f \sim 10^3$ Hz might hopefully provide coincident observations with both acoustic detectors and IFOs, based on a *different* working principle.

[5]A well known back-of-an envelope estimate (motion at the speed of light along body-horizon circumference) gives the following upper limit for the spectral content of gravitational waves originated in a process involving an accelerated mass $\sim M$: $f_{sup} \lesssim \frac{c^3}{4\pi GM} \sim 10^4 (M_\odot/M)$ [Hz] .

Before all this might come into reality, it will be necessary to build and operate one or more MAGO prototypes so that some basic issues might be efficiently addressed and solved, viz.:

- efficient decoupling from platform → suspensions design;
- efficient and quiet cooling to 1.8K → cryostat design;
- efficient readout → microwave feeding and tapping networks, and low noise amplifier design.

In parallel, a start–to–end simulation codes should be implemented, in order to tune all design parameters for best operation. In particular, criteria for obtaining the best tradeoff between detector bandwidth and noise levels should be investigated, with specific reference to selected classes of sought signals.

The present proposal is essentially focused on the above issues.

3 Detector layout

3.1 Electromagnetic design

In order to build an efficient detector, a suitable cavity shape has to be chosen. According to some general considerations, a detector based on two coupled spherical cavites looks very promising (Fig. 1) [26]. The choice of the spherical geometry is based on several factors. From the point of view of the electromagnetic design the spherical cell has the highest geometric factor G, thus it has the highest electromagnetic quality factor $\mathcal{Q}$, for a given surface resistance R_s ($\mathcal{Q} = G/R_s$). For the TE_{011} mode of a sphere, the geometric factor has a value $G \approx 850\,\Omega$, while for standard elliptical radio-frequency cavities used in particle accelerators, the TM_{010} mode has a value $G \approx 250\,\Omega$. Looking at the best reported values of surface resistance of superconducting accelerating cavities, which typically are in the $10^{-8}\,\Omega$ range, we can extrapolate that the electromagnetic quality factor of the TE_{011} mode of a spherical superconducting cavity can be $\mathcal{Q} \approx 10^{10} - 10^{11}$.

In the first generation of detectors, dedicated to the development of the experimental technique, the internal radius of the spherical cavity will be $r \approx$ 100 mm, corresponding to a frequency of the TE_{011} mode $\omega \approx 2$ GHz. The overall system mass and length will be $M \approx 5$ kg (with a wall thickness $w \approx$ 2 mm) and $L \approx 0.5$ m. The choice of the wall thickness is made considering both practical and design constraints. On one hand, the wall thickness should be kept small enough to allow an easy fabrication while maintaining sufficient stiffness to withstand the external pressure once the cavity is evacuated. Furthermore, wall thickness was chosen to optimize the cavity cooling process, and to guarantee optimum stability against point–like thermal dissipation due to possible defects present on the cavity inner surface. On the other hand, wall thickness can be used to design a particular mechanical resonant frequency and it is obviously related to the mass of the detector, which plays an important role in the signal to noise ratio.

Since this type of detector is ideally suited to explore the high frequency region of the g.w. spectrum, we plan to build a tunable cavity with 4 kHz$\leq \omega_2 - \omega_1 \leq 10$ kHz, which is outside the spectral region covered by the resonant and interferometric detectors, both existing and planned, and is still in a frequency region where interesting dynamical mechanisms producing g.w. emission are predicted [27, 28, 29].

The interaction between the g.w. and the detector is characterized by a transfer of energy and angular momentum. Since the helicity of the g.w. (the angular momentum along the direction of propagation) is 2, the g.w. can induce a transition between the two levels provided their angular momenta differ by 2; this can be achieved by putting the two cavities at right angle or by a suitable polarization of the electromagnetic field inside the resonator. The spherical cells can be easily deformed in order to induce the field polarization suitable for g.w. detection. The optimal field spatial distribution has the field axes in the two cavities which are orthogonal to each other (Fig. 6). Different spatial distributions of the e.m. field (e.g. with the field axes along the resonators' axes) have a smaller effect or no effect at all.

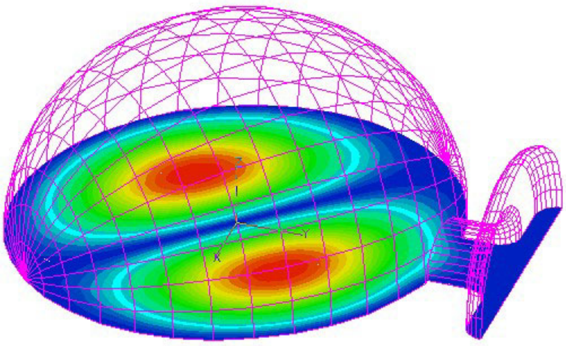

Figure 6: Electric field magnitude of the TE_{011} mode. Note the alignment of the field axis

A tuning cell is inserted in the coupling tube between the two cavities, allowing to tune the coupling strength (i.e. the detection frequency) around the design value. The dependence of the detection frequency on the distance between the two coupled cells is shown in Fig. 7, while its dependence on the diameter of the tubes is shown in Fig. 8.

One detector based on two spherical niobium cavities (with fixed coupling) has recently been built and tested at CERN (Fig. 2). A second detector with variable coupling has also been built and is now being tested (Fig. 3).

The first test on the cavity in Fig. 2, showed a quality factor $\mathcal{Q} \geq 10^{10}$ (see Fig. 9). This corresponds to a surface resistance $R_s \approx 50$ nΩ, a factor of ten higher than the best values reported for superconducting accelerating cavities. The obtained result is very satisfactory. In fact, the whole fabrication procedure (including surface treatments) is optimized for the elliptical cavity geometry used for high energy particle acceleration. Some development is still needed to tailor the technique to the spherical shape of our resonator and to obtain a surface quality comparable to that routinely obtained on elliptical cavities that would lead to a quality factor $\mathcal{Q} \approx 10^{11}$.

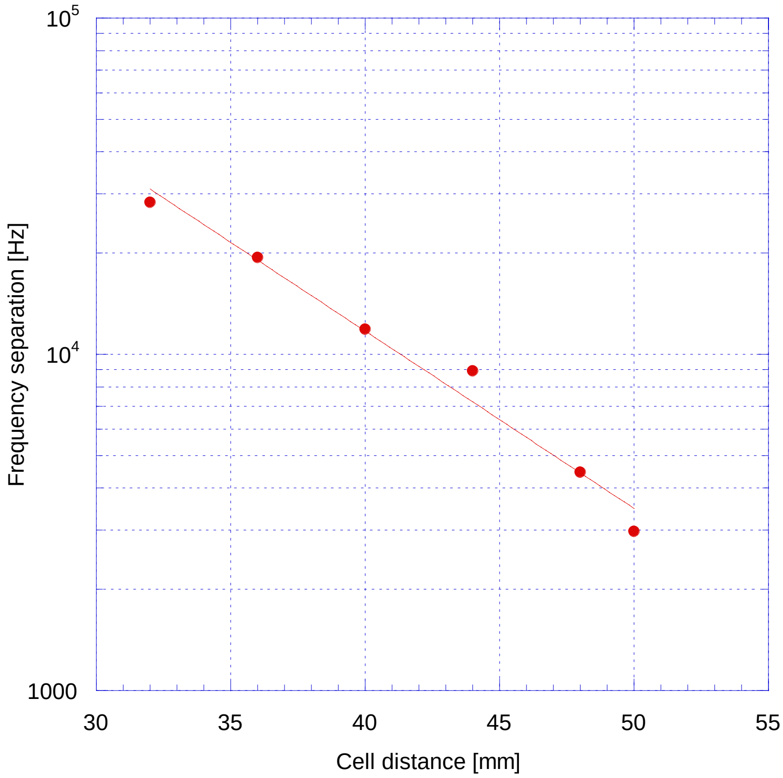

Figure 7: Detection frequency vs. coupled cells distance

3.2 Mechanical design

From the mechanical point of view it is well known that a spherical shell has the highest interaction cross-section with a g.w. and that only the quadrupolar mechanical modes of the sphere do interact with a gravitational wave [30]. The mechanical design is highly simplified if a hollow spherical geometry is used. In this case the deformation of the sphere is given by the superposition of just one or two normal modes of vibration and thus can be easily modeled. In fact, the proposed detector acts essentially as an electro–mechanical transducer; the gravitational perturbation interacts with the mechanical structure of the resonator, deforming it. The e.m. field stored inside the resonator is affected by the time–varying boundary conditions and a small quantity of energy is transferred from an initially excited e.m. mode to the initially empty one. We emphasize that our detector is sensitive to the polarization of the incoming gravitational signal. Once the e.m. axis has been chosen inside the resonator, a g.w with polarization axes along the direction of the field, will drive the energy transfer between the two modes of the cavity with maximum efficiency. With standard choices for the axes and polar coordinates, the pattern function of the detector is given by $F_\times = -\cos(\theta)\sin(2\phi)$, and is equal to the pattern function of *one* mechanical mode of a spherical resonator.

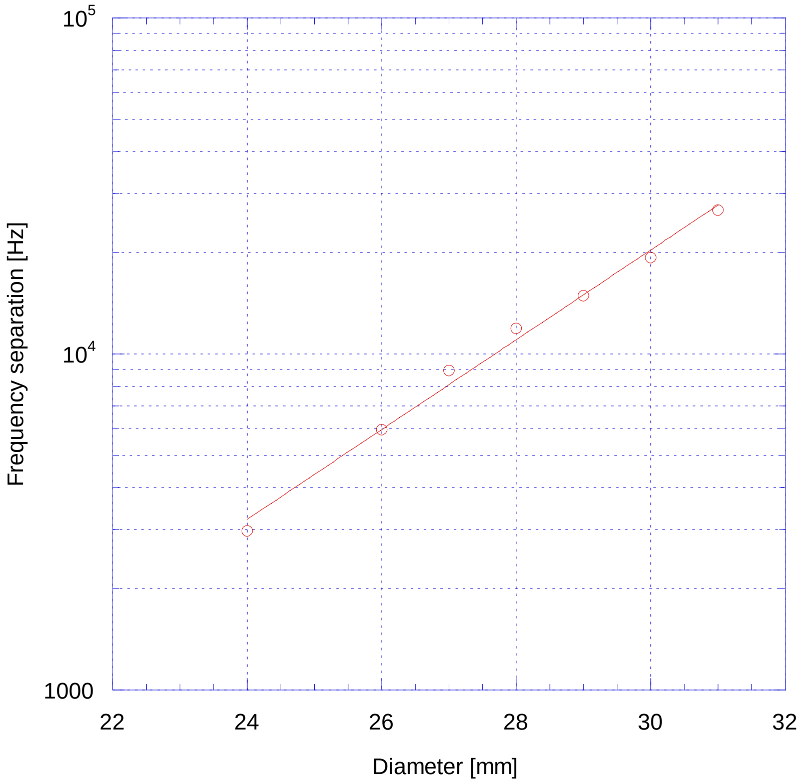

Figure 8: Detection frequency vs. coupling tubes diameter

4 Suspension system

Like a resonant bar, the whole detector must be thoroughly insulated from the environment and the mechanical design of the insulation is therefore strongly bonded with the cryogenic design. In particular, the insulation for the direct LHe supply to the cavity (see section 5) may prove to be a formidable task. The mechanical insulation foreseen for this detector may be inspired by the already existing resonant bars suspension systems, although some major differences exist.

Since one of the feature of this detector is the tunability, the mechanical design should provide adequate insulation in the frequency range 4–20 KHz and a very rough estimation suggests a minimum value of 250 dB of attenuation in the desired band (by comparison, Al bars suspension are estimated to provide $\approx$ 300 dB of insulation). A sketch of the suspension system is shown in fig. 10.

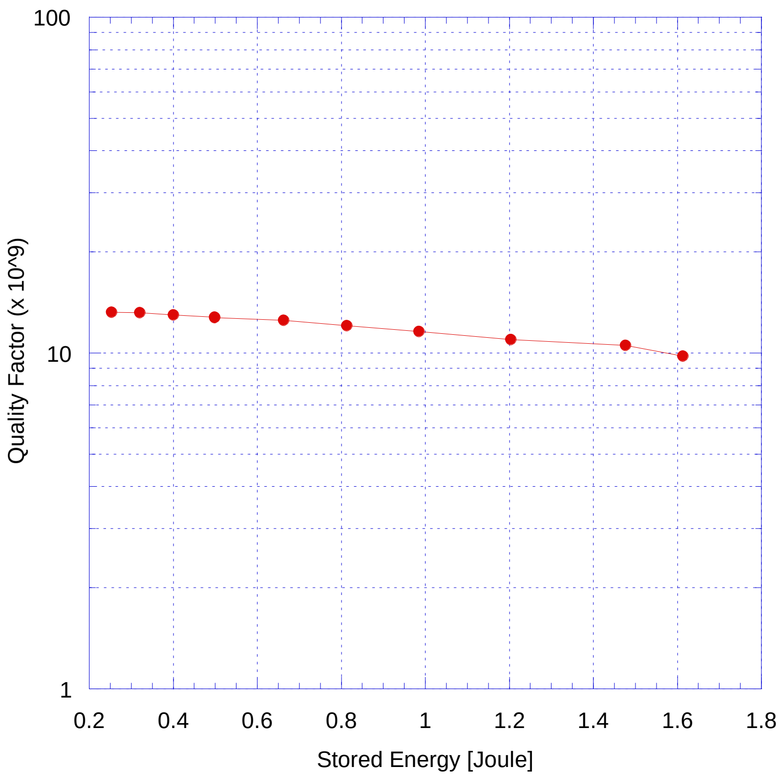

Figure 9: Quality factor vs. stored energy for the fixed–coupling cavity of Fig. 2

The room temperature filter bank is attached to the outer cryostat hull and will provide a first decoupling to the environment. There follows a cryogenic box, a facility which will host some critical low-temperature electronic components and the source for the superfluid LHe, and finally the cryogenic filter bank, which should provide the required insulation. This second stage filter is connected to the innermost cryostat, which is a superfluid LHe container hosting the detector and its tuning system. The non trivial task of filtering out environmental acoustical noise on a wide frequency band can be more easily accomplished by optimizing the two filter banks on separate frequency ranges, for example, the first stage can be optimized for low frequencies. The effectiveness of the cold filter (second stage) can be weakened by the superfluid LHe feedthrough, which runs from the cryogenic box to the MAGO cavity cryostat. Although the superfluid LHe can be conveyed by means of a suitable capillary tube, acoustic vibrations in LHe, triggered in cryo-box for instance, require a deeper understanding and maybe a dedicated damping system. The mechanical insulation design is made more complex by the MAGO cavity plus the superfluid cryostat weight. Since their weight is of the order of some tens of kilos, it is comparable to the suspensions weight and therefore, the load on uppermost suspension element can be considerably different from the lowermost one. All these problems will be addressed in the following years, where a comprehensive

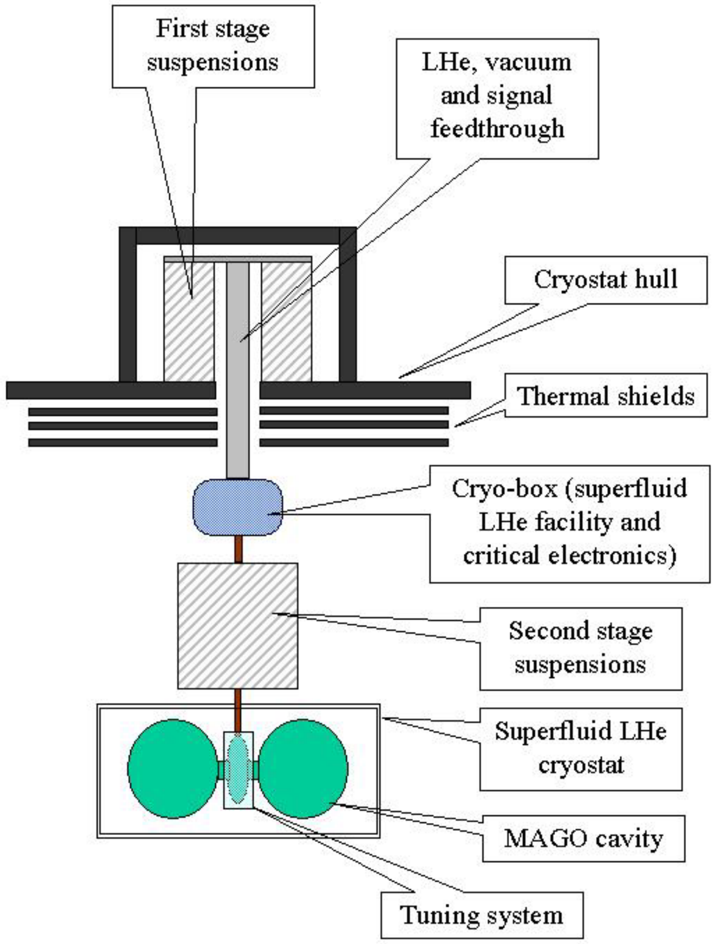

Figure 10: Sketch of the suspension system

cryogenic and mechanical design will constitute the main effort.

5 Cryogenics

Assuming the conservative value of 1 W/m^2 for the super–insulation radiation losses, the radiating heat load is $P_{rad} \approx 4$ W. Adding to this figure a couple of watts to account for the conduction losses in the cavity suspension (tie–rods), we obtain the value of $P_{tot} \approx 6$ W as an upper limit. These steady state losses have to be compared with the RF cryogenic losses of our detector.

Assuming, in operation, a peak surface magnetic field $H_{surf} = 0.1$ T (half of the critical field of niobium) the stored energy in the cavity will be $U \approx 30$ J. We remark that $H_{surf} = 0.1$ T corresponds (in an accelerating cavity) to 25 MV/m of accelerating field, a value routinely achieved in the cavities developed for the

Tesla project. Given the geometric factor of our cavity, $G = 835\ \Omega$, and assuming a residual surface resistance of 5 nΩ (the surface resistance routinely obtained in the LEP–II cavities at 1.8 K), we can foresee a quality factor $\mathcal{Q} \approx 10^{11}$, corresponding to a dissipation of 4 W in the helium bath (@ $H_{surf} = 0.1$ T).

The planned operating temperature of our system is 1.8 K to fully exploit the advantages of the RF superconductivity. At the chosen frequency of 2 GHz the surface resistance at 1.8 K is well saturated at the residual value, avoiding the change of surface resistance produced by the heating of the surface. The use of superfluid helium as refrigerant guarantees a very good thermal dissipation for the cavity, with an even temperature distribution along the cavity surface.

To further improve the heat exchange and reduce the effect of the helium boil–off we propose a scheme of refrigeration similar to the one foreseen for the LHC magnets and already used since the eighties for the refrigeration of high field magnets (e.g. TORE–II supra). The flow chart of the refrigerator is shown in figure 11.

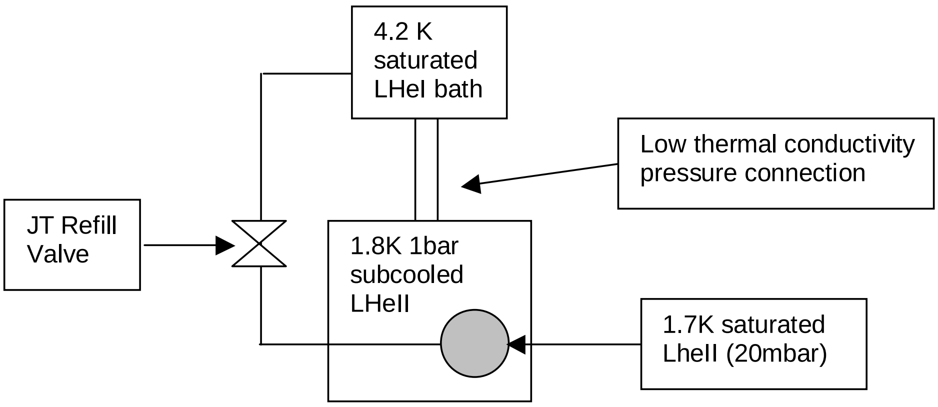

Figure 11: Flow chart of the subcooled superfluid helium refrigerator

This refrigeration scheme, using subcooled superfluid helium, at atmospheric pressure and 1.7–1.8 K, avoids all the problems related to the bubbles in the refrigerating bath, improves the Kapitza resistance at the helium–cavity wall interface and increases by 30% the peak transfer value to the helium bath. This refrigeration scheme will be the best solution also from the point of view of the mechanical noise induced on the detector by the LHe bath. The subcooled operation at 1.8 K and atmospheric pressure (compared with saturated helium at 1.8 K and 20 mbar), will eliminate the possibility of the bubble gas production. This effect of an abrupt reduction of the bath induced mechanical noise below the helium λ–point was already experienced on Weber type gravitational detectors [31].

To form a bubble of a certain size in subcooled helium we need not only to transfer to the helium bath the amount of heat corresponding to the heat of vaporization, but also the enthalpy needed to reach the normal boiling point of the gas at 4.2 K. Furthermore the Claudet–type refrigerator reduces to a minimum the refrigerator–bath interaction minimizing the mechanical noise coming from the pumps and from the saturated HeI bath. The sub–atmospheric HeII bath cools the main bath only by conduction via the heat exchanger HT, the refill of this bath is done trough the JT needle valve working on the liquid helium flow. The hydraulic impedance of this needle is quite high and damps any pressure fluctuation due to the pumping system. The 4.2 K bath is in hydraulic contact with the 1.8 K sub–cooled bath via the high impedance duct to reduce the heat input to the superfluid helium and allows to reduce the bath temperature well below the λ–point of the helium (2.19 K). To obtain this result we need a quite long and narrow hydraulic channel with a very high thermal impedance, but also the hydraulic impedance of the channel is high, decoupling the superfluid bath from the saturated (4.2 K) or nearly superfluid bath. In this way pressure fluctuations due to the He bath refilling or to turbulences, produced by thermo–acoustic oscillations of the saturated bath, will have a negligible effect on the superfluid bath.

Coming to the conclusions the proposed refrigeration scheme will greatly help in reducing the sensitivity of the proposed detector to the acoustic noise produced by the fluctuation of the helium bath wile giving us the more comfortable situation by the point of view of the RF performances.

6 Detection electronics

The three main functions of rf control and measurement system of the experiment are:

1. The first task of the system is to lock the rf frequency of the master oscillator to the resonant frequency of the symmetric mode of the cavity and to keep constant the energy stored in the mode. The frequency lock of the master oscillator to the cavity mode is necessary to fill in energy in the fundamental mode of the cavity. The reduction of fluctuations of the stored energy to less than 100 ppm greatly reduces the possibility of ponderomotive effects due to the radiation pressure of the electromagnetic field on the cavity walls and helps to minimize the contribution of the mechanical perturbations of the resonator to the output noise. The frequency lock allows also to design a detection scheme insensitive to fluctuations of the resonant frequency of the two cavities forming our detector.

2. The second task is to increase the detector's sensitivity by driving the coupled resonators purely in the symmetric mode and receiving only the rf power up–converted to the antisymmetric mode by the perturbation of the cavity walls. This goal can be obtained by rejecting the signal at the symmetric mode frequency taking advantage of the symmetries in the field distribution of the two modes. Our system, despite of some additional complexity, guarantees the following improvements over the one used in previous experiments:

    - a better rejection of the phase noise of the master oscillator obtained using the sharp resonance ($Q = 10^{10}$) of the resonator as a filter;

- a better insulation of the drive and detector ports obtained by using separate drive and detection arms of the rf system;
- the possibility of an independent adjustment of the phase lag in the two arms giving a better magic–tee insulation at the operating frequencies;
- a greater reliability for the frequency amplitude loop using the transmitted power, instead of the reflected, coming from the cavity.

3. The third task is the detection of the up–converted signal achieving the detector sensitivity limit set by the contribution of the noise sources [32]. Slow pressure fluctuations on the cooling bath, hydrostatic pressure variations due to the changes in the helium level, pressure radiation, and so on, will change in the same way the resonant frequency of both modes. Using a fraction of the main oscillator power as local oscillator for the detection mixer, the detection system becomes insensitive to frequency drifts of both modes, allowing for a narrow band detection of the up–converted signal produced by the cavity wall modulation.

6.1 The rf control loop

The RF signal generated by the master oscillator (HP4422B) is fed into the cavity through a TWT amplifier giving a saturated output of 20 Watt in the frequency range 2–4 GHz. The energy stored in the cavity is adjusted at the operating level by controlling the output of the master oscillator via the built–in variable attenuator.

The output signal is divided by a 3 dB power splitter. The A output of the splitter is sent to the TWT amplifier, the B output is sent, through the phase shifter (PS), to the local oscillator (LO) input of a rf mixer acting as a phase detector (PD). The output of the rf power amplifier is fed to the resonant cavity through a

double directional coupler, and a 180^o hybrid ring acting as a magic–tee. The rf power enters the magic–tee via the sum arm, Σ, and is split in two signals of same amplitude and zero relative phase, coming out the tee co–linear arms 1 and 2.

The rf signal, reflected by the input ports of the cavity, enters the magic–tee through the co–linear arms. The two signals are added at the Σ arm and sampled by the directional coupler to give information about the energy stored in cavity allowing for the measurement of the coupling factor, quality factor, stored energy. While driving the cavity on the symmetric mode no reflected signal is shown at the Δ port of the magic–tee where the signals coming from the co–linear arms are algebraically added to zero due to the 180^o phase shift.

To get the maximum of the performances of the magic–tee we need to have equal reflected signals (phase and amplitude) at the cavity input ports. To preserve the signal integrity we use matched lines (in phase and amplitude) inside the cryostat. Because the phase shift is very sensitive to temperature inhomogeneities between the two cables and the phase difference between the two co–linear arms of the magic–tee gives a quite strong signal at the Δ port, we need to compensate for differential thermal contractions of the cables inside the cryostat, leading to phase unbalance in the feed lines. To do that we insert a phase shifter in one of the lines to compensate for differences and to reduce to a minimum the leakage of the unwanted modes on the two ports. As we will show in section 6.2, mode leakage of the symmetric mode to the Δ port sets a limit to the system sensitivity increasing the overall noise level of the detector.

Mode leakage of the antisymmetric mode to the Σ port reduces the system sensitivity by reducing the signal level available for detection. The output ports of the cavity are coupled for a maximum output signal on the antisymmetric mode (detection mode) and the magic–tee is used to reject the rf power at the frequency of the symmetric mode. A fraction of the signal at the Σ port is fed to the rf input of the phase detector PD via a low noise rf amplifier. The intermediate frequency (IF) output of the phase detector PD is fed back to the rf master oscillator to lock the output signal to the resonant frequency of the resonator. The total phase shift around the loop is set through the phase shifter PS, to have the maximum energy stored in the detector. A careful design of the servo loop amplifier (SLA) guarantees the stability of the system and the rejection of the residual noise of the master oscillator up to one MHz. The same fraction of the Σ output of the output magic–tee is used to keep constant, to 100 ppm, the energy stored in the cavity feeding back an error signal to drive the electronically controlled output attenuator of the master oscillator.

Great deal of care is needed in tailoring the frequency response of both controls because the two loops can interact producing phase–amplitude oscillations in the rf fields stored in the cavities.

6.2 Sensitivity enhancement using the mode symmetry

The two modes of the detector cavity have (as in the case of two coupled pendula) opposite symmetries of the fields.

Using two separate sets of ports to drive the cavity and to receive the up–converted signal at the frequency of the antisymmetric mode, the cavity acts as a very sharp filter (due to the high Q), with an high rejection of the noise coming from the master oscillator at the frequency of the up–converted signal. This already low residual noise, can be even more reduced in our scheme using two magic–tees to drive the cavity purely in the symmetric mode and to detect only the up–converted energy, rejecting the unwanted field components by an amount given by the magic–tee insulation.

In the case of an ideal magic–tee the mode rejection is infinite. If the cavity is driven purely in the symmetric mode no symmetric mode component is transmitted through the system and there will be no signal at the output port. In the ideal case this result is obtained also in the more simple scheme used by Melissinos and Reece [33, 34], measuring the up–converted power coming out of the detector along the input lines.

Our scheme gives better sensitivity and performances in the real case. The first obvious gain is the sum of the Δ and Σ port insulation of the two tees, plus the possibility of adjusting separately the input and output lines to get better mode rejection. In a commercial magic–tee the insulation is specified to be $\approx 25 - 35$ dB over its own bandwidth. The reason for this quite low insulation is mainly due to the difficulty of balancing on a large range of frequency the phases of the signals coming from the two co–linear arms of the tee.

A phase unbalance as small as five degrees reduces the insulation from Δ to Σ port to only 25 dB.

Our electronic scheme allows for an independent compensation of the magic–tee phase mismatch both at the feed frequency and at the detection frequency in a flexible way: the phase mismatch is compensated using a variable phase shifter at the input of one of the co–linear arms. The optimum phase at the input side results in a pure excitation of the symmetric (drive) mode, keeping the power at the frequency of the antisymmetric (detection) mode 70 dB below the level of the drive mode. Adjusting the phase at the output will couple only the antisymmetric mode component, rejecting the symmetric mode component by 70 dB. The total symmetric–antisymmetric mode rejection of the system is the sum of the attenuation we can obtain from the two 180^o hybrids.

The input and output ports of the two cell cavity need to be critically coupled ($\beta = 1$) to the rf source and to the rf detection system. In this way we have the optimum transfer of power to the symmetric mode (a maximum of stored energy) and to the antisymmetric mode (a maximum in the detector output). Because the frequency and field distribution of the two modes are quite close, the input and output ports are critically coupled to both modes. For that reason 50% of the symmetric mode signal is coupled to the idle Σ port at the output magic–tee,

and symmetrically 50% of the antisymmetric mode signal is coupled to the idle Δ port at the input magic–tee. We remark that, since those two ports are not used in our detection scheme, it is necessary to reflect back into the cavity the energy flowing out of them. This task is achieved by a proper termination of the ports; a careful analysis showed that closing the ports with an open circuit completely decouples the input and output arms (optimum rejection of the symmetric mode) and maximizes the stored energy and the detector sensitivity.

At the Σ port of the detection arm we insert a directional coupler to sample a tiny amount of the symmetric mode power coming from the cavity. This signal is fed into the frequency–amplitude servo loop used to lock the master oscillator to the cavity frequency and to keep constant the energy stored in the cavity.

6.3 Detection of the converted signal

Having devised a means of suppressing the high level pump frequency signal, the remaining problem is to amplify and detect the low level parametric mode signal. The detection limit, hence overall sensitivity of the machine is now determined by the RF thermal noise level. In order to detect the low level signal it must be amplified and to do this without degrading the signal to noise ratio, a low noise amplifier is required. The lower the effective noise figure of the RF amplifier, the higher will be the sensitivity. In this case we can make use of the fact that the resonant cavities are operated at cryogenic temperatures and use a cryogenic low noise amplifier with lowest possible noise figure.

Since the late 1970s research has been conducted into the performance of GaAs FET and later GaAs HEMT RF amplifiers at cryogenic temperatures. The principle applications for this technology have been for radio astronomy receivers and for satellite ground station receivers. A typical receiver uses a 2 stage closed cycle Helium refrigerator reach a base temperature of around 15 K. HEMT amplifiers work well at this temperature if carefully design, but can also work down to liquid Helium temperatures. However, the additional benefit in noise temperature performance of operating at LHe compared to 15 K is not great and is mostly not justified when traded-off against of system complexity, when the equipment must operated in a radio astronomy telescope or a satellite ground station antenna. However, in this application, cooling to 4.5 K or 1.5K in liquid Helium is available in the same dewar as the superconducting coupled cavities.

The layout of the detection electronics is shown in fig. 12.

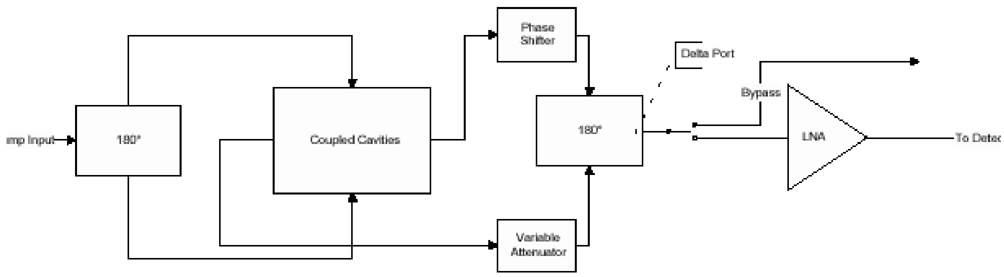

Figure 12: Electric circuit of the detector system

The signal converted to the antisymmetric mode by the interaction between the mechanical perturbation and the rf fields is coupled to the Δ port of the detection arm of the rf system and amplified by the low noise rf amplifier LNA.

The converted rf signal amplified by the LNA is fed to the rf input port (RF) of a low noise double balanced mixer M1; the local oscillator port (LO) of M1 is driven by the symmetric mode rf power (at angular frequency ω_s). The LO input level is adjusted to minimize the noise contribution from the mixer. As shown in the previous section the input spectrum to the RF port of the mixer consists of two signals: the first at angular frequency ω_s coming from the rf leakage of the symmetric mode through the detection system; the second is the converted energy at angular frequency ω_a. Both signals are down–converted by the M1 mixer giving to the IF port a DC signal proportional to the symmetric mode leakage and a signal at angular frequency Ω proportional to the antisymmetric mode excitation. The down–converted IF output is further amplified using a low noise audio preamplifier.

For the detection electronics of mechanically coupled interactions, at angular frequency Ω, as gravitational waves, since the exact frequency and phase of the driving source is not known, we can't perform a synchronous detection. We need to perform an auto–correlation of the detector output,

or to cross–correlate the outputs of two different detectors.

The outlined detection scheme gives the benefit of being insensitive to perturbations affecting in the same way the frequency of the two modes.

The first point to note in terms of the general architecture of the solution is that if a cryogenic amplifier is to be used within the same cryogenic dewar as the coupled cavities, then the phase shifter, variable attenuator and 180^o hybrid also need to be inside the dewar. If this is not the case then the noise temperature contribution of these components will dominate and there will be little, if any, benefit in having a cooled amplifier. As it is known that HEMT amplifiers can be produced for cryogenic operation, we shall first focus on the passive components. A consequence of placing the phase shifter and variable attenuator inside the cryogenic dewar is that they will have to be controllable by an electrical signal, rather than manually. For this reason the description below considers voltage controlled devices. In the interest of implementing a solution which is reasonably economic, the preferred approach will be to use commercial devices for the passive components, rather than developing special–to–type components. Many electronic components, particularly passive ones, will operate at cryogenic temperatures, even if not specified to do so by their manufacturers. Hence, the following focuses on the potential problems which will need to be investigated in order to qualify commercial components.

The 180^o hybrid is essentially a just a strip line device. The only concern about operation in cryogenic temperatures is due to differential thermal contraction of the materials of the component, particularly in the area of the connections between the strip line and coaxial I/O connectors. There may also be changes in dielectric properties of the substrate, which may affect the impedance of the I/O ports. Nevertheless strip line couplers have been used in many cryogenic applications without any problem, so we shall only validate this component with a simple test.

Voltage controlled phase shifter. The key element of the shift shifter is a varactor diode. Silicon and GaAs diodes are know to be capable of operation at cryogenic temperatures. However, particularly in the case of silicon, the electrical characteristics change significantly at cryogenic temperatures. Therefore, it is predicted that a phase shifter will still operate a cryogenic temperatures but its transfer characteristics will change significantly from the ambient temperature specifications. For this reason a particular aim will be to calibrate the device when operating at cryogenic temperatures. Another factor to note is that varactor diode phase shifters have limitations in operating power. Between 0 dBm and + 5dBm input power the varactor diodes begin to work as rectifiers. In any case, the pump energy in the cavity output ports is typically below 0dBm, but this should be confirmed.

Voltage controlled variable attenuator. The key element of a voltage variable attenuator is a diode and so the analysis given above for the phase shifter is also relevant for the variable attenuator.

Bypass Switch. The function of the bypass switch is to allow coarse tuning of the circuit for pump frequency suppression. Before the phasing is tuned the pump frequency signal may be large and could saturate the low noise amplifier. The bypass switch will allow for direct connection of a spectrum analyser outside the dewar for initial tuning. The bypass switch will be coaxial relay type.

7 Response of the detector

7.1 Signal

The interaction between the stored e.m. field and the time–varying boundary conditions depends on both how the boundary is deformed by the external perturbation and on the spatial distribution of the fields inside the resonator. Any field configuration inside the resonator can be expressed as the superposition of the electromagnetic normal modes [35]: $\mathbf{E}(\mathbf{r},t) = \sum \mathcal{E}_n(t)\,\mathbf{E}_n(\mathbf{r})$; $\mathbf{H}(\mathbf{r},t) = \sum \mathcal{H}_n(t)\,\mathbf{H}_n(\mathbf{r})$, with $\mathcal{E}_n(t) \equiv \sqrt{\epsilon_0}\int \mathbf{E}\cdot\mathbf{E}_n\,dV$; $\mathcal{H}_n(t) \equiv \sqrt{\mu_0}\int \mathbf{H}\cdot\mathbf{H}_n\,dV$ and $\int \mathbf{H}_n\cdot\mathbf{H}_m\,dV = \int \mathbf{E}_n\cdot\mathbf{E}_m\,dV = \delta_{nm}$.

Similarly if $\mathbf{u}(\mathbf{r},t)$ denotes the displacement of the mass element of the walls at point $\mathbf{r}$ and time t, relative to its position at rest, the displacement of the walls can be written as the superposition of the mechanical normal modes $\boldsymbol{\xi}_\alpha(\mathbf{r})$ [36]: $\mathbf{u}(\mathbf{r},t)=\sum \boldsymbol{\xi}_\alpha(\mathbf{r})\, q_\alpha(t)$, with $\int \boldsymbol{\xi}_\alpha(\mathbf{r})\cdot\boldsymbol{\xi}_\beta(\mathbf{r})\rho(\mathbf{r})\,dV = M\delta_{\alpha\beta}$, where M and ρ are the mass and the density of the walls.

We want to study the energy transfer between two electromagnetic normal modes of a resonator whose boundary is perturbed by an external force when mode "1" is highly excited by an external source at its eigenfrequency, $\mathcal{H}_1 \approx A_1\cos(\omega_1 t)$ and $\mathcal{E}_1 \approx A_1\sin(\omega_1 t)$, with *constant* amplitude A_1. We shall assume that only one mechanical mode couples to the external force. Including empirical damping terms, the equations of motion for the field amplitudes are given by:

$$\ddot{\mathcal{H}}_2 + \frac{\omega_2}{\mathcal{Q}}\dot{\mathcal{H}}_2 + \omega_2^2\mathcal{H}_2 = -\frac{1}{2}\,\omega_2^2 q_m C_{21}^m \mathcal{H}_1 \tag{1}$$

$$\ddot{q}_m + \frac{\omega_m}{Q_m}\,\dot{q}_m + \omega_m^2 q_m = \frac{f_m}{M} - \frac{1}{2}\frac{C_{21}^m}{M}\,\mathcal{H}_2\mathcal{H}_1^* \tag{2}$$

where $f_m(t)=\int \mathbf{f}(\mathbf{r},t)\cdot\boldsymbol{\xi}_m(\mathbf{r})\,dV$, and $\mathbf{f}(\mathbf{r},t)$ is the volume force density which acts on the walls. The time–independent coupling coefficient C_{21}^m is given by (the superscript m labels the *mechanical* normal mode, while the subscripts label the *electromagnetic* modes):

$$C_{21}^m = \int_S (\mathbf{H}_2\cdot\mathbf{H}_1 - \mathbf{E}_2\cdot\mathbf{E}_1)\,\boldsymbol{\xi}_m\cdot d\mathbf{S}\,. \tag{3}$$

The dependence of the coupling coefficient, and therefore of the energy transfer, both on the field spatial distribution and on the boundary deformation, has been checked using a resonator made up of two pill–box cavities, mounted *end–to–end* and coupled by a small circular aperture in their common endwall. The perturbation of the resonator's boundary was induced by two piezoelectric crystals mounted in the center of the two circular endwalls. The TE_{011} symmetric mode at 3 GHz was excited by an external rf source and the piezos were driven by a synthesized oscillator tuned at the frequency corresponding to the symmetric–antisymmetric mode separation (≈ 500 kHz). The relative phase of the signals driving the two piezos could be set to 0 degrees and to 180 degrees with an external switch. Eq. 3 predicts for this field and for this boundary configuration $C_{21}^m = 0$, for the in-phase excitation and $C_{21}^m = 2$, for the excitation with 180 degrees phase lag. These predictions are clearly confirmed by the data shown in Fig. 13. The explicit calculation of the coupling coefficient C_{21}^m for an arbitrary deformation of the resonator volume can be done only by numerical methods. Analytic calculations showed that for an ideal spherical hollow resonator, excited in the fundamental quadrupolar mechanical mode and in the TE_{011} electromagnetic mode, $C_{21}^m = 1.9$. More detailed calculations, made on a realistic model of the coupled spheres, including the central coupling cell and the e.m. input and output ports, were made by finite element methods.

$\mathcal{H}_2(t)$ is given by:

$$\mathcal{H}_2(t) = \int_0^\infty K(\tau) f_m(t-\tau)\,d\tau = \frac{1}{2\pi}\int_{-\infty}^{+\infty} \widetilde{K}(\omega)\widetilde{f}_m(\omega)\exp(i\omega t)\,d\omega\,; \qquad K(\tau)=0 \text{ for } \tau \le 0\,. \tag{4}$$

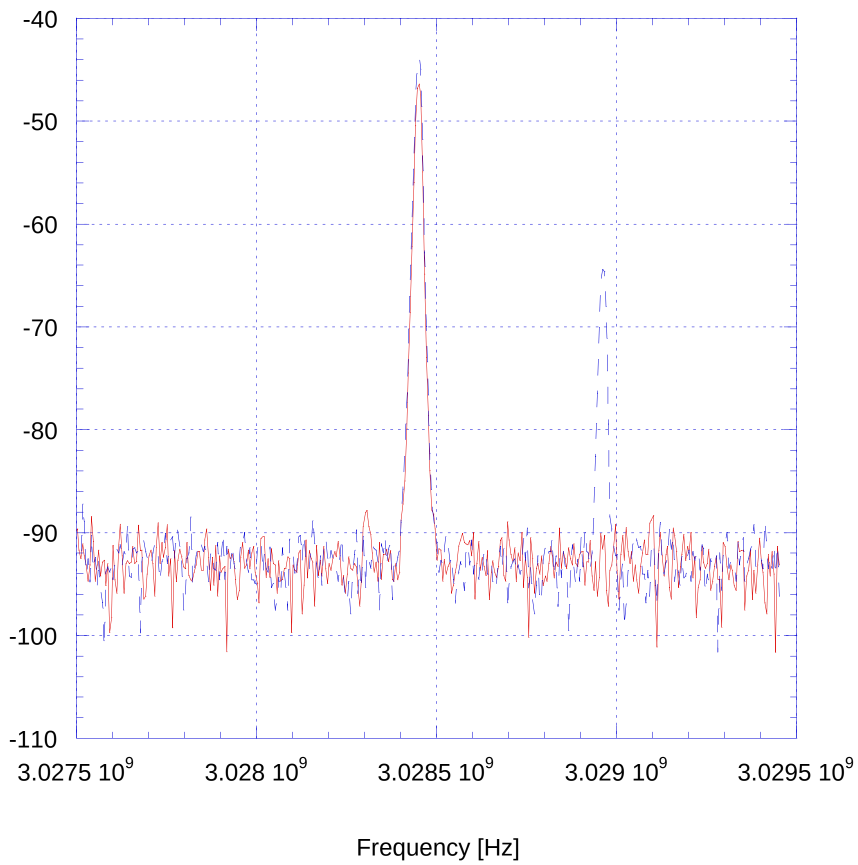

Figure 13: Power trasfer between the symmetric and the antisymmetric mode with in–phase piezo excitation (solid) and 180 degress out–of–phase excitation (dashed)

The density of the external forces driving the motion of the system, i.e. the tides generated by the passing gravitational wave, are given by

$$f_i(\mathbf{r},t) = -\rho(\mathbf{r}) R_{0i0j}(t) x^j \ , \tag{5}$$

where ρ is the wall density, and $R_{0i0j}(t)$ are the components of the Riemann tensor evaluated in the center of mass of the solid. The components of the Riemann tensor can be expressed in terms of the adimensional amplitude of the g.w. $R_{0i0j}(t) = -1/2\,\ddot{a}_{ij}(t)$.

For a "+" polarized plane g.w travelling along the z axis the force density, in the proper reference frame attached to a detector lying in the xy plane, has the form:

$$\mathbf{f}(\mathbf{r},t) = \frac{1}{2}\rho(\mathbf{r})\ddot{a}(t)\,[-x, y, 0] \ , \tag{6}$$

with a similar expression for the "×" polarization. The generalized force, acting on the m mechanical mode, then has the form

$$f_m(t) = -\frac{1}{2}\,\ddot{a}(t)\int_{Vol}[(\xi_m)_x\,x - (\xi_m)_y\,y]\,\rho(\mathbf{r})\,dV\,. \tag{7}$$

$\widetilde{f}_m(\omega)$ is then given by:

$$\widetilde{f}_m(\omega) = \frac{1}{2}\,M\omega^2\mathcal{L}\,\widetilde{a}(\omega) \tag{8}$$

having defined the detector's effective length (for this mechanical mode and wave polarization):

$$\mathcal{L} = \frac{1}{M}\int_{Vol}[(\xi_m)_x\,x - (\xi_m)_y\,y]\,\rho(\mathbf{r})\,dV \tag{9}$$

The function $\widetilde{K}(\omega)$ is found to be:

$$\widetilde{K}(\omega) = \frac{C_{21}^m\omega_2^2 A_1/(2M)}{\left[\omega_2^2 - (\omega+\omega_1)^2 + i\,\frac{\omega_2}{\mathcal{Q}}(\omega+\omega_1)\right]\left[\omega_m^2 - \omega^2 + i\,\frac{\omega\omega_m}{Q_m}\right] - \frac{(C_{21}^m A_1\omega_2)^2}{4M}}\,\exp(i\,\omega_1 t) \tag{10}$$

The second term in the denominator of Eq. 10 is due to the back–action of the electromagnetic fields on the cavity walls. Its effect is particularly important when $\omega_2 - \omega_1 \approx \omega_m$. In this case optimum signal transfer does not correspond to the maximum field amplitude A_1 that can be stored in the initially excited mode (that is limited by the critical field of the superconductor, $H_c \approx 0.2$ T for niobium). Instead, optimum signal transfer is obtained from a lower value that has to be optimized according to the prevailing experimental conditions and detector characteristics. The dependence of the signal on the energy stored in the initially excited mode will be further discussed in Section 6.2 where the expected sensitivity of the detector in various experimental conditions is analyzed.

The average energy stored in mode number 2 is $U_2 = 1/2|\mathcal{H}_2(t)|^2$ and the power extracted from a cavity port coupled to an external load with a coupling coefficient β_2 is $P_2 = \beta_2\,(\omega_2/\mathcal{Q})\,U_2$.

If $a(t) = h\alpha(t)$ with $\alpha(t)$ periodic at angular frequency Ω, the expression of the output power from mode 2 is given by $P_2 = \mathcal{R}(\Omega)\,h^2$, with

$$\mathcal{R}(\Omega) = \frac{1}{4}\,\frac{\beta_2\omega_2}{\mathcal{Q}}\,\Omega^4 M^2\mathcal{L}^2|\widetilde{K}(\Omega)|^2\,. \tag{11}$$

7.2 Noise

To study how the thermal fluctuations of the walls contribute to the output signal, we will start again from Eqs. 1–2, taking now the external force $f_m(t)$ as a stochastic force with constant power spectrum $S_{fm} = 4Mk_BT\omega_m/Q_m$ [37]. The output noise power spectral density is given by:

$$S_{PP}(\omega) = \frac{\beta_2\omega_2}{\mathcal{Q}}\,|\widetilde{K}(\omega)|^2 S_{ff} \tag{12}$$

The thermal fluctuations of the electromagnetic field itself can be calculated in an analogus way. Starting again from Eqs. 1–2, we consider an external, stochastic force coupled to the magnetic field $\mathcal{H}_2(t)$, with constant power spectrum $S_{fe} = 4kT/(\omega_2\mathcal{Q})$. The output noise spectral density is given by:

$$S_{\mathcal{H}\mathcal{H}} = \frac{\beta_2\omega_2}{\mathcal{Q}} |\widetilde{\chi}(\omega)|^2 S_{fe} \tag{13}$$

with $\widetilde{\chi}(\omega)$ given by:

$$\widetilde{\chi}(\omega) = \frac{\omega_2^2\left(\omega_m^2 - \omega^2 + i\,\frac{\omega\omega_m}{Q_m}\right)}{\left[\omega_2^2 - (\omega+\omega_1)^2 + i\,\frac{\omega_2}{\mathcal{Q}}(\omega+\omega_1)\right]\left[\omega_m^2 - \omega^2 + i\,\frac{\omega\omega_m}{Q_m}\right] - \frac{(C_{21}^m A_1\omega_2)^2}{4M}}\,. \tag{14}$$

We note that in the limit of vanishing coupling, $C_{21}^m \approx 0$, the contribution to the output noise of the walls vanishes, while the contribution of the electromagnetic field fluctuations tends to be like a simple harmonic oscillator of frequency ω_2 and quality factor $\mathcal{Q}$.

Other noise sources must also be taken into account. To operate our device we have to feed microwave power into mode 1, using an external rf source locked on mode 1, at frequency ω_1. The master oscillator phase noise is filtered through the resonator linewidth; the power spectral density has the following frequency dependence [35]:

$$S_{MO}(\omega) = \frac{4\beta_1 P_i/(\omega_1\mathcal{Q})}{\left(\frac{1}{\mathcal{Q}}\right)^2 + \left(\frac{\omega+\omega_1}{\omega_1} - \frac{\omega_1}{\omega+\omega_1}\right)^2} \tag{15}$$

where P_i is the power input level and β_1 is the coupling coefficient of mode 1 to the output load. From the above equation we can estimate the microwave power noise spectral density at the detection frequency $\omega = \omega_2 - \omega_1$:

$$S_{MO}(\omega_2 - \omega_1) \approx \beta_1 \frac{P_i}{\omega_1\mathcal{Q}}\left(\frac{\omega_2}{\omega_2 - \omega_1}\right)^2 \tag{16}$$

This figure can be improved if the receiver discriminates the spatial field distribution of the e.m. field at frequency ω_2, i.e. if it is sensitive only to the power excited in mode number 2, rejecting all contributions coming from mode number 1. In this way mode 1 is decoupled from the output load and $\beta_1 = 0$. The experimental set–up, based on the use of two magic–tees which accomplishes this issue, is discussed in detail in [5]. Of course, the mode discrimination cannot be ideal, and some power leaking from mode 1 to the detector's output will be present. Nevertheless our previous work has demonstrated that with careful tuning of the detection electronics we can obtain $\beta_1 \leq 10^{-14}$ [5].

The input Johnson noise of the first amplifier in the detection electronics has to be added to the previous contributions to establish the overall noise spectral density. It can be described by the frequency independent spectral density [37]:

$$S_{JJ} = k_B T(10^{(N/10)} - 1) \equiv k_B T_{eq} \tag{17}$$

where N is the noise figure of the amplifier (in dB) and T the operating temperature. The equivalent temperature (or noise temperature) T_{eq}, is equal to the temperature (in Kelvin) of a 50 ohm termination at the input of an ideal noiseless amplifier with the same gain and generating the same output noise power.

Other noise sources (e.g. the seismic noise) are not considered in this paper.

We shall characterize the noise in our detector by a frequency dependent spectral density $S_h(\omega)$, with dimension Hz^{-1} defined as

$$S_h(\omega) = \frac{S_n(\omega)}{\mathcal{R}(\omega)} \tag{18}$$

where $S_n = S_{PP} + S_{\mathcal{H}\mathcal{H}} + S_{MO} + S_{JJ}$, is the detector noise spectral density.

7.3 Sensitivity

Let us focus our attention on the system based on two spherical niobium cavities working at $\omega_1 \approx \omega_2 \approx 2$ GHz with a maximum stored energy in the initially excited symmetric mode of $U_1 \approx 10$ J per cell (corresponding to a maximum surface magnetic field $H_{max} = 0.1$ T, half the critical field of niobium). This is a small–scale system with an effective length of 0.1 m and a typical weight of 5 kg. The lowest quadrupolar mechanical mode is at $\omega_m \approx 4$ kHz. In the following, we shall consider an equivalent temperature of the detection electronics $T_{eq} = 1$ K.

A possible design of the detector uses both the mechanical resonance of the structure, and the e.m. resonance. Due to the tuning system, the detection frequency can be made equal to the mechanical mode frequency $\omega_m \approx \omega_2 - \omega_1$. The expected sensitivity of the detector for $\omega_2 - \omega_1 = \omega_m = 4$ kHz is shown in figure 14, for a mechanical quality factor $Q_m = 10^3$ (solid line) and $Q_m = 10^6$ (dashed line). Note that, in the two cases, the optimum sensitivity is obtained with different values of stored energy. In both cases the stored energy has been optimized for maximum detector bandwidth. When the mechanical quality factor is higher ($Q_m = 10^6$) the stored energy has to be maintained much under the maximum allowed value.

When $\omega_2 - \omega_1 = \omega_m$, the detector sensitivity is limited by the walls thermal motion. In this case, a lower T_{eq} would increase the detection bandwidth.

Since our detector is based on a double resonant system (the mechanical resonator and the electromagnetic resonator) it can be operated also for frequencies $\omega_2 - \omega_1 \neq \omega_m$. At frequencies $\omega_2 - \omega_1 \leq 1$ kHz the master oscillator phase noise will, in general, completely spoil the system sensitivity, while at frequencies $\omega_2 - \omega_1 \geq 10$ kHz the noise coming from the detection electronics will dominate. The expected sensitivity of the small–scale detector for $\omega_2 - \omega_1 = 10$ kHz is shown in figure 15.

In order to increase the expected sensitivity a large–scale system has to be developed. A possible design could be based on two spherical cavities working at $\omega_1 \approx \omega_2 \approx 500$ MHz, with $\omega_m \approx 1$ kHz. This system could have a maximum stored energy of $U_1 \approx 1200$ J per cell, an effective length of 0.4 m and a typical weight of 2300 kg. With a reasonable choice of system parameters one could obtain the sensitivity shown in figure 16, for the double-resonance case ($\omega_2 - \omega_1 = \omega_m$). As in the previous (small–scale) case the energy store in the initially excite mode has been optimized for maximum bandwidth, and it has to be much less then the maximum allowed. Also in this case lowering T_{eq} corresponds to an increase of the detection bandwidth.

Obviously the large–scale system could also be used at higher frequencies; in this case a good sensitivity can be achieved in a narrow detection bandwidth (see Fig. 17).

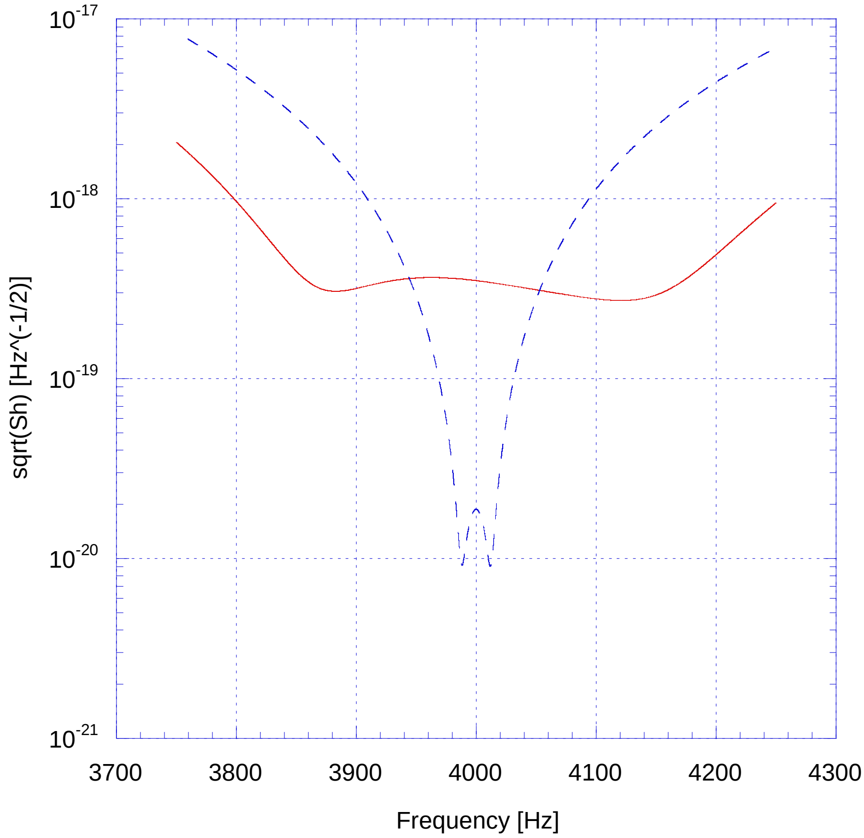

Figure 14: Calculated system sensitivity ($\omega_m \approx \omega_2 - \omega_1 \approx 4$ kHz, $\mathcal{Q} = 10^{10}$, $T = 1.8$ K, $T_{eq} = 1$ K, and a) $Q_m = 10^3$, stored energy $U \approx 10$ J per cavity (solid line); b) $Q_m = 10^6$, stored energy $U \approx 0.1$ J per cavity (dashed line))

It is worth noting that the narrow detection bandwidth is not an unavoidable drawback of the system. Actually its value is determined by the coupling coefficient of the antisymmetric mode at the Δ port of the output magic–tee, and can be adjusted changing this coupling. This corresponds to changing (lowering) the quality factor of the antisymmetric mode, leaving the quality factor of the symmetric mode unaffected. Of course an increased bandwidth corresponds to a lower sensitivity, since the latter is proportional to the antisymmetric mode quality factor. The possibility to increase the detection bandwidth is also interesting for other possible applications of this detection technique which is based on the parametric frequency conversion between two electromagnetic modes in a cavity (for example, in connection with recently proposed detectors based on the dual resonator concept [38, 39, 40]).

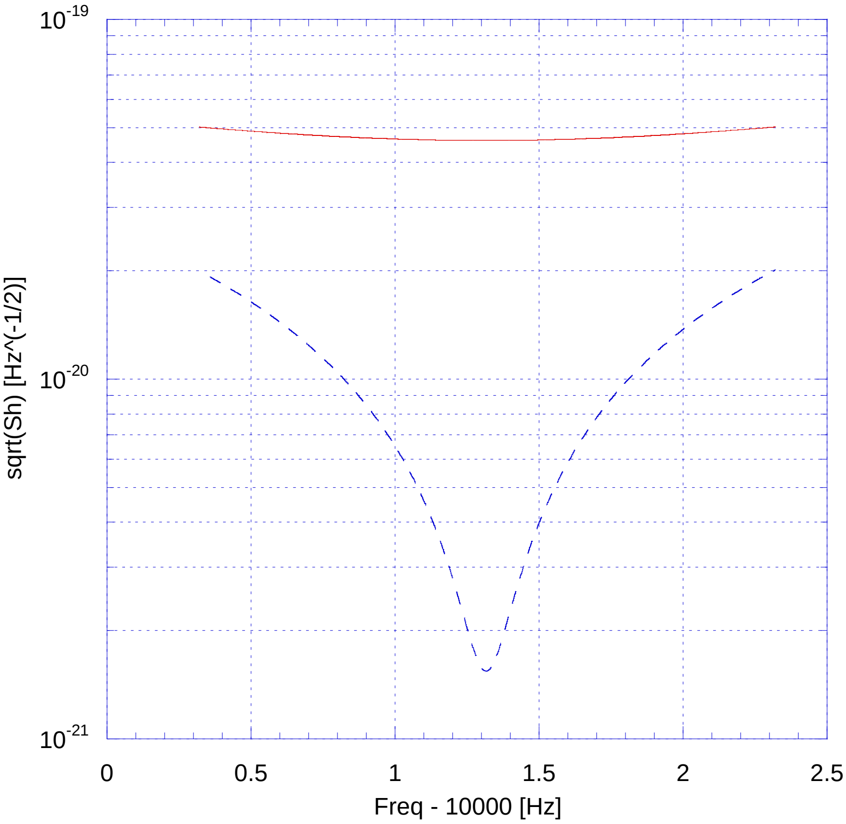

Figure 15: Calculated system sensitivity ($\omega_m \approx 4$ kHz, $\omega_2 - \omega_1 \approx 10$ kHz, $\mathcal{Q} = 10^{10}$, $T = 1.8$ K, $T_{eq} = 1$ K, stored energy $U \approx 10$ J per cavity and a) $Q_m = 10^3$ (solid line); b) $Q_m = 10^6$ (dashed line))

8 Data analysis

Several aspects of MAGO data analysis need to be investigated.

The data-analysis for both single and multiple MAGOs will be akin of those used for acoustic detectors [41], in view of the narrowband MAGO response.

Data analysis strategies for MAGOs operating above $f \sim 4 \cdot 10^3$ Hz will be strictly *non parametric*, in view of the present lack of GW source/signal models in this frequency range.

Optimum MAGO tuning schedules for detecting unknown (sub)millisecond pulsars [42], [43] will be obviously a most relevant issue to be investigated.

A "xylophone" of MAGOs tuned in the range between 10^3 Hz and 10^4 Hz might be able to *both* detect *and estimate* the chirp-mass [44] of galactic light[6] BH-MACHO binaries [45], which would produce a distinct signature in the xylophone output [46]. The expected (optimistic) event-rate might be non negligible

[6] The highest GW frequency radiated during binary inspiral is twice the orbital frequency of the last stable circular orbit, and is [44] $f \sim 4 \cdot 10^3 (M_\odot/M)$ [Hz] .

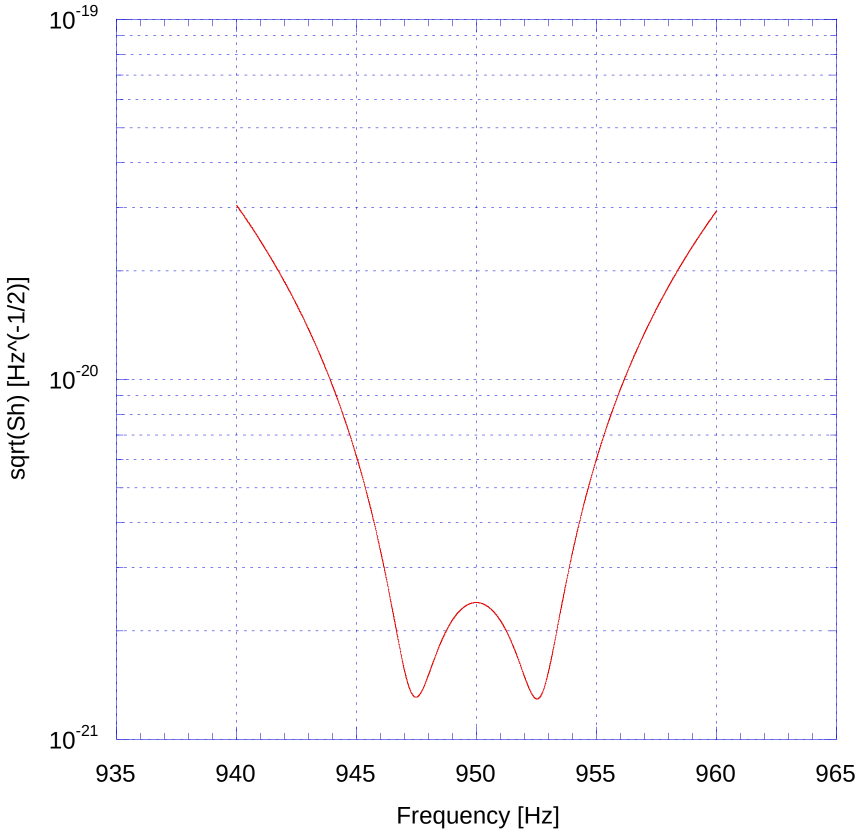

Figure 16: Calculated system sensitivity ($\omega_m \approx \omega_2 - \omega_1 \approx 1$ kHz, $\mathcal{Q} = 10^{10}$, $Q_m = 10^6$, $T = 1.8$ K, $T_{eq} = 1$ K, stored energy $U \approx 1$ J per cavity)

[41].

Once MAGO prototypes will be up and running, a primary task will be to investigate the experimental noise PSD and transfer function, by comparison to their theoretical counterparts.

The MAGO data-analysis activity will be initially focused on the above mentioned issues.

9 Collaboration, cost and schedule

9.1 Collaboration

- *INFN–Genova*

  People: R. Ballantini, A. Chincarini, S. Cuneo, G. Gemme (spokeperson), R. Parodi, E. Picasso, R. vaccarone (4.2 FTE in 2004).

  Tasks: Suspension system. Refrigerator and cryostat. Low noise electronics. Rf tests.

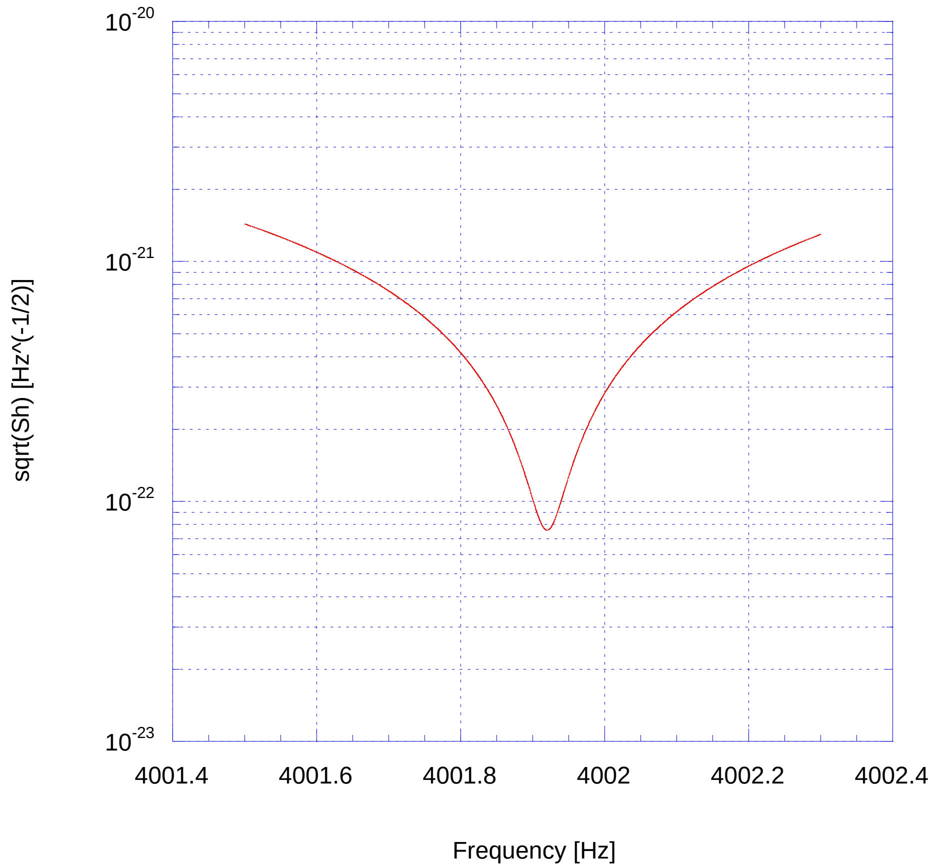

Figure 17: Calculated system sensitivity ($\omega_m \approx 1$ kHz, $\omega_2 - \omega_1 \approx 4$ kHz, $\mathcal{Q} = 10^{10}$, $Q_m = 10^6$, $T = 1.8$ K, $T_{eq} = 1$ K, stored energy $U \approx 1200$ J per cavity)

- *CERN*[1] People: Ph. Bernard, E. Chiaveri, S. Calatroni, R. Losito (0.9 FTE).

  Tasks: Refrigerator and cyostat. Rf simulations and tests.

- *INFN–Napoli (Gruppo Collegato di Salerno)*

  People: R.P. Croce, V. Galdi, V. Pierro, I.M. Pinto (local coordinator) (1 FTE).

  Tasks: Source modelling. Data analysis. Rf simulations and tests.

9.2 Cost

An overview of the costs of the experiment is given in table 9.2. Their subdivision (including missions and consumables) in the years 2004–2007 is given in table 9.2.

[1]CERN does not tale part in the experiment as an external institution.

System	Item	Cost (k€)
Cryostat	Vessels	200
	Refrigerator	180
Suspension system		220
Read–out electronics and data acquisition		200
Total		800

Table 1: Cost estimation (hardware and constructions)

Year	2004	2005	2006	2007	Total
Cost (k€)	230	330	450	350	1360

Table 2: Cost subdivision (including missions and consumables)

9.3 Schedule and subdivision of tasks

In the first two years (2004–2005) the main effort will be dedicated to the design, construction and test of critical components of the system. In the first year the layout of the suspension system will be designed and a prototype of an element of each stage will be produced, preceeded by a thorough analysis of their behaviuor by finite element calculations. Obviously we shall take advantage of the wide experience gained by the groups that have been working on this item for several decades. INFN–Genova group will be in charge of this task.

The study of the suspension system has to be worked out in parallel with the design of the subcooled superfluid helium refrigerator, which should provide the cooling power needed to maintain the cavity at low temperature, without introducing an unacceptable amount of noise from the external environment. We have identified two critical components of the refrigerator, which have to be designed and tested in the first couple of years. First, the automatic control of the saturated superfluid helium level in the saturated superfluid helium box. Second, the channel connecting the saturated helium bath at 4.2 K with the vessel housing the detector. This component provides a direct connection between the inner vessel, which houses the detector, and the external enviroment. For this reason it needs to be integrated with the suspension system, and has to be studied carefully, both from the thermal and from the mechanical point of view. Our goal is to complete the design of the cryostat in the third quarter of 2005 and to start the commissioning of its components by the end of 2005. INFN–Genova group, together with the CERN group, will be in charge of this task.

In the first two years, the detection elecronics has to be characterized, together with the suspension and refrigeration systems. The first task will be the construction of a cryogenic test–bed for the measurement of the noise figure of amplifiers, rf passive components, and their combinations. The system should consist of a dual variable temperature insert (VTI). One VTI is needed for the components under test, the other for the source resistor.

The first half of 2004 will be devoted to the construction of the test facility. In the second half of 2004 we shall start with the characterization of the chosen LNA. The contribution to the noise power spectral density coming from the amplifier should be less than the intrinsic noise generated in the cavity. We estimate that this noise level corresponds to that of an amplifier with a noise temperature of 1 K. Standard GaAS microwave amplifiers for satellites and communication will be studied at low temperature. No data for commercial amplifiers operating below 77 K are available. A sizable noise reduction should be obtained working at 4.2 K or below, but the actual amount reduction has to be found.

At Chalmers University the group of Prof. H. Zirath is leader in the production of HEMT made with InP technology. Their amplifiers are optimized for 4 GHz and beyond, where the noise temperature is about 2.5 K. The noise at 2 GHz is slightly higher. We plan to study their device at 4.2 K and below, and to have the amplifier optimized for 2 GHz use. Other devices using transistors manufactured by ETH and TRW have been tested for the Herschel project. Even in this case the band and noise are optimized for 4–8 GHz use. A noise temperature of 3.5 K has been attained at a temperature of 13 K.

An essential role in the detection system is played by a few passive components, which are needed to subtract the opposite signal coming from the two cavities. To reach a good null condition we have to correct the fase and the amplitude of the two channels. The nulling condition must be modified in real time by a control loop, with a time constant of the order of the milliseconds. We will have to find or to develop cryogenic components like magic–Tees, electrically variable attenuators and phase shifters. At low temperature the use of ferroelectric materials is promising. Another technology is based on MEMS, and is preferred when the parameter must be changed digitally. During the second year (2005) we shall characterize the low temperature behaviour of passive rf components (phase shifters, attenuators, ecc.). INFN–Genova group, together with INFN–Napoli group, will be in charge of the characterization of the detection electronics.

The development of reliable models of candidate sources of gw's is a formidable task, together with the study of the most effective data analysis strategies to extract their signal from the detector's noise. This issues will be carried on in parallel with the experimental effort. INFN–Napoli group will be in charge of this task.

Year 2006 will be mainly dedicated to the construction of the cryostat, while in 2007 the whole system shall be integrated and tested.

References

[1] http://www.roma1.infn.it/rog/
http://www.lnl.infn.it/ auriga/welcome.html
http://gravity.phys.lsu.edu/
http://www.gravity.pd.uwa.edu.au/.

[2] http://www.virgo.infn.it/
http://www.ligo.caltech.edu/
http://www.geo600.uni-hannover.de/
http://tamago.mtk.nao.ac.jp/tama.html
http://lisa.jpl.nasa.gov/.

[3] F. Pegoraro, L.A. Radicati, Ph. Bernard, and E. Picasso. Electromagnetic detector for gravitational waves. *Physics Letters*, 68A(2):165–168, 1978.

[4] F. Pegoraro, E. Picasso, and L.A. Radicati. On the operation of a tunable electromagnetic detector for gravitational waves. *Journal of Physics A*, 11(10):1949–1962, 1978.

[5] Ph. Bernard, G. Gemme, R. Parodi, and E. Picasso. A detector of small harmonic displacements based on two coupled microwave cavities. *Review of Scientific Instruments*, 72(5):2428–2437, 2001. arXiv:gr-qc/0103006.

[6] R. Ballantini, Ph. Bernard, E. Chiaveri, A. Chincarini, R. Losito, G. Gemme, R. Parodi, and E. Picasso. A detector of high frequency gravitational waves based on coupled microwave cavities. *Classical and Quantum Gravity*, 2003. To be published.

[7] A.J. Farmer and E.S. Phinney. astro-ph/0304393.

[8] M.G. Haehnelt. *Mon. Not. Roy. Astron. Soc.*, 269:199, 1994.

[9] F.D. Ryan. *Phys. Rev. D*, 52:5707, 1995.

[10] http://lisa.jpl.nasa.gov; http://sci.esa.int/home/lisa/.

[11] V. Kalogera et al. *Astrophys. J. Lett.*, 550, 2001.

[12] A. Burrows and J. Hayes. *Phys. Rev. Lett.*, 76:352, 1996.

[13] B.J. Owen et al. *Phys. Rev. D*, 58:084020, 1998.

[14] B. Allen and J.D. Romano. *Phys. Rev. D*, 59:102001, 1999.

[15] http://vega.ess.sci.osaka-u.ac.jp/gwdaw/files/0401.pdf.

[16] http://gravity.phys.lsu.edu/.

[17] http://www.auriga.lnl.infn.it/.

[18] http://www.roma1.infn.it/rog/explorer/explorer.

[19] http://www.lnf.infn.it/esperimenti/rog/nautilus.

[20] http://www.gravity.pd.uwa.edu.au.

[21] L.S. Finn and S. Mukherjee. *Phys. Rev. D*, 63:062004, 2001.

[22] S. M. Merkowitz and W. W. Johnson. *Physical Review D*, 51:2546, 1995.

[23] http://www.minigrail.nl.

[24] P. Astone et al. *Nucl. Phys. Proc. Suppl.*, 70:461, 1999.

[25] O.D. Aguiar et al. *Class. Quantum Grav.*, 19:1949, 2002.

[26] Ph. Bernard, A. Chincarini, G. Gemme, R. Parodi, and E. Picasso. In *Proceedings of the X^{th} Workshop on Rf Superconductivity*, Tsukuba, Japan, 2001. http://conference.kek.jp/SRF2001/pdf/PZ001.pdf.

[27] B. Schutz. The case for broadband high frequency detectors. In *Gravitational waves advanced detectors workshop (GWADW)*, Aspen, (CO), 2003.

[28] K.D. Kokkotas and N. Andersson. Oscillation and instabilities of relativistic stars. In *Recent developments in general relativity*, Milan, Italy, 2002. Springer–Verlag. Proc. of the XIV Conference of general relativity and gravitational physics, Genoa, 2000.

[29] K.D. Kokkotas. High frequency gravitational waves sources. Proc. of the Amaldi 5 International Conference on Gravitational Waves, Tirrenia, 2003.

[30] J.A. Lobo. What can we learn about gw physics with an elastic spherical antenna? *Physical Review D*, 52:591, 1995.

[31] P. Astone et al. Noise behaviour of the Explorer gravitational wave antenna during λ transition to the superfluid phase. *Cryogenics*, 32(7):668, 1992.

[32] Ph. Bernard, G. Gemme, R. Parodi, and E. Picasso. Coupled microwave cavities for the detection of small harmonic displacements. Technical Report INFN/TC–98/17, INFN, 1998.

[33] C.E. Reece, P.J. Reiner, and A.C. Melissinos. Observation of 4×10^{-17} cm harmonic displacement using a 10 GHz superconducting parametric converter. *Physics Letters*, 104A(6,7):341, 1984.

[34] C.E. Reece, P.J. Reiner, and A.C. Melissinos. Parametric converters for detection of small harmonic displacements. *Nuclear Instruments and Methods*, A245:299–315, 1986.

[35] J.C. Slater. *Microwave Electronics*. D. Van Nostrand Company, Inc., New York, 1950.

[36] P.R. Saulson. Thermal noise in mechanical experiments. *Physical Review D*, 42(8):2437–2445, 1990.

[37] A. Papoulis. *Probability, Random Variables and Stochastic Processes*. McGraw–Hill, New York, 1965.

[38] M. Cerdonio et al. Wideband dual spere detector of gravitational waves. *Physical Review Letters*, 87:031101, 2001.

[39] L. Conti et al. A wideband and sensitive gw detector for khz frequencies: The dual sphere. *Classical and Quantum Gravity*, 19:2013–2019, 2002.

[40] M. Bonaldi et al. Selective readout and back-action reduction for wideband acoustic gravitational wave detectors. 2003. arXiv:gr-qc/0302012.

[41] L.S. Finn. Gravitational radiation sources and signatures. arXiv:gr-qc/9903107, 1999.

[42] J. Cordes and D.F. Chernoff. *Astrophys J.*, 482:971, 1997.

[43] L. Burderi et al. astro-ph/0109088, 2001.

[44] L.S. Finn. *Phys. Rev. D*, 53:2878, 1996.

[45] T. Nakamura et al. *Astrophys . Lett.*, 487, 1997.

[46] R.P. Croce et al. 2003.

List of Figures

List of Tables

Codice	Esperimento	Gruppo
	MAGO	2
Rapp. Naz.: Gianluca Gemme		

ISTITUTO NAZIONALE DI FISICA NUCLEARE

Preventivo per l'anno ***2004***

PREVISIONE DI SPESA

Piano finanziario globale di spesa

In KEuro

ANNI FINANZIARI	Miss. interno	Miss. estero.	Materiale di cons.	Trasp. e Facch.	Spese Calc.	Affitti e Manut. Appar.	Mater. inventar	Costr. appar.	TOTALE Compet.
2004	*35*	*59*	*25*	*0*	*0*	*17.5*	*71.5*	*28*	***236.0***
2005	35.0	50.0	25.0	0.0	0.0	17.5	90.5	112.0	***330.0***
2006	35.0	50.0	25.0	0.0	0.0	17.5	122.5	200.0	***450.0***
2007	35.0	50.0	75.0	0.0	0.0	17.5	72.5	100.0	***350.0***
TOTALI	***140,0***	***209,0***	***150,0***			***70,0***	***357,0***	***440,0***	***1366,0***

Mod EC./EN. 6 (a cura del responsabile nazionale)

ISTITUTO NAZIONALE DI FISICA NUCLEARE

Preventivo per l'anno ***2004***

Codice	Esperimento	Gruppo
	MAGO	2
Resp. loc.: Innocenzo Pinto		

Struttura
SA

COMPOSIZIONE DEL GRUPPO DI RICERCA

N	RICERCATORE Cognome e Nome	Qualifica: Dipendenti Ruolo	Dipendenti Art. 23	Incarichi Ricerca	Incarichi Assoc.	Affer. al gruppo	%
1	Croce Rocco P.				AsRic	2	20
2	Galdi Vincenzo			P.A.		2	20
3	Pierro Vincenzo			P.A.		4	30
4	Pinto Innocenzo			P.O.		4	30

Numero totale dei ricercatori **4**

Ricercatori Full Time Equivalent **1**

N	TECNOLOGI Cognome e Nome	Qualifica: Dipendenti Ruolo	Dipendenti Art. 23	Incarichi Ass. Tecnol.	%

Numero totale dei Tecnologi **0**

Tecnologi Full Time Equivalent **0**

N	TECNICI Cognome e Nome	Qualifica: Dipendenti Ruolo	Dipendenti Art. 15	Incarichi Collab. tecnica	Incarichi Assoc. tecnica	%

Numero totale dei Tecnici **0**

Tecnici Full Time Equivalent **0**

SERVIZI TECNICI

	Denominazione	mesi-uomo

Annotazioni:

Osservazioni del direttore della struttura in merito alla disponibilità di personale e attrezzature

Mod EC./EN. 7 (a cura del responsabile locale)

ISTITUTO NAZIONALE DI FISICA NUCLEARE

Preventivo per l'anno ***2004***

Codice	Esperimento	Gruppo
	MAGO	2
Rapp. Naz.: Gianluca Gemme		

MILESTONES PROPOSTE PER IL 2004

Data completamento	Descrizione
30/6/2004	Disegno elementi della sospensione
30/6/2004	Completamento test−bed per la qualifica dei componenti elettronici
31/12/2004	Prototipo elemento sospensione
31/12/2004	Test elementi critici refrigeratore
31/12/2004	Test LNA (GaAs e InP) a 4.2K e 1.8K

Mod EC./EN. 8 (a cura del responsabile nazionale)

ISTITUTO NAZIONALE DI FISICA NUCLEARE

Preventivo per l'anno ***2004***

Codice	Esperimento	Gruppo
	OPERA	2
Rapp. Naz.: Muciaccia Maria Teresa		

Rappresentante nazionale: Muciaccia Maria Teresa
Struttura di appartenenza: BA
Posizione nell'I.N.F.N.:

INFORMAZIONI GENERALI	
Linea di ricerca	Fisica del neutrino:ricerca oscillazioni nm − nt per long base line
Laboratorio ove si raccolgono i dati	L.N.G.S.
Sigla dello esperimento assegnata dal laboratorio	OPERA/CNGS1
Acceleratore usato	SPS del CERN
Fascio (sigla e caratteristiche)	fascio di neutrini muonici CNGS
Processo fisico studiato	Rivelazione di oscillazioni. nm − nt tramite l'identificazione diretta del leptone tau prodotto in reazioni di corrente carica del neutrino−tau
Apparato strumentale utilizzato	Apparato ibrido: bersaglio di piombo ed emulsioni nucleari complementato da rivelatori elettronici e spettrometri per muoni
Sezioni partecipanti all'esperimento	BARI, FRASCATI, LNGS,L'AQUILA, NAPOLI, ROMA1, SALERNO, BOLOGNA, PADOVA
Istituzioni esterne all'Ente partecipanti	IIHE (BRUSSEL), ITEP (MOSCA),JINR (Dubna), BERN UNIVERSITY,Neuchatel, LYON UN., HAIFA, METU ANKARA, AICHI UN. (GIAPPONE), TOHO UN. (GIAPPONE), KOBE UN. (GIAPPONE), NAGOYA UN. (GIAPPONE), UTSONOMYA (GIAPPONE), LAPP (ANNECY), MUNSTER UN,IHEP (PECHINO), BERLINO, HAGEN, AMBURGO,ROSTOCK, IPNL (LIONE),LAL(Orsay), STRASBURGO, ZAGABRIA
Durata esperimento	1999 (preparazione) − 2010

ISTITUTO NAZIONALE DI FISICA NUCLEARE

Preventivo per l'anno **2004**

Codice	Esperimento	Gruppo
	OPERA	2
Resp. loc.: Giuseppe Grella		

Struttura
SA

PREVENTIVO LOCALE DI SPESA PER L'ANNO 2004

In KEuro

VOCI DI SPESA		DESCRIZIONE DELLA SPESA	IMPORTI Parziali	SJ	Totale Compet.	SJ	A cura della Comm.ne Scientifica Nazionale
Viaggi e missioni	Interno	Riunioni di collaborazione (7.8 kE) e project board (1.2 kE).	9.0		**34.0**	**0.0**	
		Riunioni analisi.	3.5				
		Preparazione laboratorio e test al LNGS.	10.0				
		Attività RDmicroscopi.	11.5				
	Estero	Riunione di collaborazione in europa (5.8 kE) + 3 riunioni di coordinamento al CERN (3 kE)	8.8		**50.5**	**0.0**	
		Riunione di collaborazione in Giappone.	7.2				
		Riunioni analisi (6.3 kE); RDmicroscopi (8 kE).	14.5				
		Test beam e test al CERN.	20.0				
Materiale Consumo		Metabolismo in sede.	7.5		**44.5**	**0.0**	
		Laboratorio microscopi.	19.0				
		Consumo al CERN ed al LNGS.	15.0				
		Assemblaggio microscopio.	3.0				
Trasp. e facch.					**0.0**	**0.0**	
Spese Calcolo		Consorzio / Ore CPU / Spazio Disco / Cassette / Altro			**0.0**	**0.0**	
Affitti e manutenz. apparecchiat.					**0.0**	**0.0**	
Materiale inventariabile					**0.0**	**0.0**	
Costruzione Apparati		Prototipo per apparecchio per griglitura emulsioni (con ROMA1).	10.0		**72.0**	**0.0**	
		Costruzione microscopio.	62.0				
			Totale		**201.0**	**0.0**	

Sono previsti interventi e/o impiantistica che ricadono sotto la disciplina della legge Merloni ? ☐

Breve descrizione dell'intervento:

Mod EC./EN. 2 (a cura del responsabile locale)

ISTITUTO NAZIONALE DI FISICA NUCLEARE

Preventivo per l'anno ***2004***

Codice	Esperimento	Gruppo
	OPERA	2
Resp. loc.: Giuseppe Grella		

Struttura
SA

ALLEGATO MODELLO EC2

Attività svolte nel 2003:

1) E' in funzione un primo prototipo di microscopio capace di effettuare lo scanning delle emulsioni con velocità di circa 10 cm2/ora con efficienze di scansione attorno al 95% sui dati raccolti con i test beam effettuati presso il CERN. Parallelamente sono in fase di sviluppo gli algoritmi necessari alla realizzazione del tracking asincrono in parallelo allo scopo di aumentare la velocità di scansione. Si stanno effettuando test con Matrox Odyssey e CMOS veloci.

2) Test − beam al CERN con emulsioni finali di OPERA.

3) Studio di fattibilità del metodo di grigliaggio (riferimenti e numerazione delle emulsioni) con fibre ottiche, led etc.

4) Test vari di sviluppo di emulsioni al CERN finalizzati anche allo studio ed al dimensionamento del laboratorio da costruire al LNGS.

ISTITUTO NAZIONALE DI FISICA NUCLEARE

Preventivo per l'anno ***2004***

Struttura
SA

Codice	Esperimento	Gruppo
	OPERA	2
Resp. loc.: Giuseppe Grella		

ALLEGATO MODELLO EC2

(a cura del responsabile locale)

ISTITUTO NAZIONALE DI FISICA NUCLEARE

Preventivo per l'anno ***2004***

Codice	Esperimento	Gruppo
	OPERA	2
Rapp. Naz.: Muciaccia Maria Teresa		

PREVENTIVO GLOBALE DI SPESA PER L'ANNO 2004

In KEuro

Struttura	A CARICO DELL' I.N.F.N.																		A carico di altri Enti
	Miss. interno	di cui **SJ**	Miss. estero.	di cui **SJ**	Materiale di cons.	di cui **SJ**	Trasp. e Facch.	di cui **SJ**	Spese Calc.	di cui **SJ**	Affitti e Manut. Appar.	di cui **SJ**	Mater. inventar.	di cui **SJ**	Costr. appar.	di cui **SJ**	TOTALE Compet.	di cui **SJ**	
AQ																			0,0
BA	52,0		88,0		29,5										810,0	700,0	979,5	700,0	0,0
BO	58,5		52,5		29,5										86,0		226,5		0,0
LNF	214,5	25,0	126,5	30,0	135,5		10,0						15,0		4078,0	200,0	4579,5	255,0	0,0
LNGS	19,0		30,5		147,5		5,0								247,0		449,0		0,0
NA	106,0		167,0		119,5								25,0		345,0		762,5		0,0
PD	106,5		58,5		77,5		20,0						5,0		495,0		762,5		0,0
RM1	30,5		27,5		54,5										162,0		274,5		0,0
SA	34,0		50,5		44,5										72,0		201,0		0,0
TOTALI	**621,0**	**25,0**	**601,0**	**30,0**	**638,0**		**35,0**						**45,0**		**6295,0**	**900,0**	**8235,0**	**955,0**	

NB. La colonna A carico di altri enti deve essere compilata obbligatoriamente

Note:

Mod EC./EN. 4 (a cura del responsabile nazionale)

ISTITUTO NAZIONALE DI FISICA NUCLEARE

Preventivo per l'anno ***2004***

Codice	Esperimento	Gruppo
	OPERA	2
Rapp. Naz.: Muciaccia Maria Teresa		

A) ATTIVITA' SVOLTA FINO A GIUGNO 2003

Spettrometri: iniziato montaggio Maggio 2003, a Settembre montaggio lastre e RPC.
Wall: eseguiti test su prototipi, gara chiusa a Settembre 2003.
Struttura supporto: bandita gara a Maggio 2003.
RPC: produzioni iniziata Gennaio, prodotte 300 camere (1/3 totale).
Inizio produzione delle strip di lettura.
Emulsioni : Preparazione infrastrutture al LNGS e CERN.Test di trattamento e qualita'.Test con cosmici.Test al PS per idetificazione e/pai.
Microscopi: completato il tuning del prototipo a 10 cm2/h con efficienze di tacciamento attorno al 95% e in fase di ulteriore miglioramento.
Installati ed operativi microscopi per la misura dei test beam nei vari laboratori di scanning. In fase di test lo scanning a 20 cm2/h.
BAM : test su brick sottovuoto, preselezione ditte e gara entro Novembre 2003.

B) ATTIVITA' PREVISTA PER L'ANNO 2004

Spettrometri : completamento e accensione primo magnete. Inizio montaggio secondo magnete.
Wall : Inizio consegna settembre 2004. Studi su posizionamento brick.
Struttura supporto: istallazione per primo e secondo magnete.
RPC : installazione nel primo e secondo magnete.
Emulsioni : immagazzinamento emulsioni a LNGS,prototipo per catena automatizzata per sviluppo, test con cosmici ed esposizione a fasci di circa 100 brick.
Microscopi : Installazione primo microscopio in versione finale in ciacun laboratorio,
misure test beam, installazione delle infrastutture e di parte dei microscopi per la stazione di scanning per i CS.
BAM : controllo costruzione BAM in ditta.

C) FINANZIAMENTI GLOBALI AVUTI NEGLI ANNI PRECEDENTI *In kEuro*

Anno finanziario	Missioni interno	Missioni estero	Materiale di consumo	Trasp. e Facch.	Spese Calcolo	Affitti e Manut. Apparec.	Materiale inventar.	Costruz. apparati	***TOTALE***
2002	216.5	499.5	573.5	15.0	0.0	0.0	201.5	1225.0	2731.0
2003	321.0	229.5	775.5	42.5	0.0	0.0	382.5	2202.0	3953.0
TOTALE	**537.5**	**729**	**1349**	**57.5**	**0**	**0**	**584**	**3427**	**6684**

Mod EC. 5 (a cura del rappresentante nazionale)

ISTITUTO NAZIONALE DI FISICA NUCLEARE

Preventivo per l'anno ***2004***

Codice	Esperimento	Gruppo
	OPERA	2
Rapp. Naz.: Muciaccia Maria Teresa		

PREVISIONE DI SPESA

Piano finanziario globale di spesa

In KEuro

ANNI FINANZIARI	Miss. interno	Miss. estero.	Materiale di cons.	Trasp. e Facch.	Spese Calc.	Affitti e Manut. Appar.	Mater. inventar	Costr. appar.	TOTALE Compet.
2004	*621*	*601*	*638*	*35*	*0*	*0*	*45*	*6295*	***8235.0***
2005	750.0	600.0	950.0	100.0	0.0	0.0	500.0	5000.0	***7900.0***
2006	750.0	500.0	950.0	100.0	0.0	0.0	500.0	2000.0	***4800.0***
TOTALI	***2121,0***	***1701,0***	***2538,0***	***235,0***			***1045,0***	***13295,0***	***20935,0***

Mod EC./EN. 6 (a cura del responsabile nazionale)

ISTITUTO NAZIONALE DI FISICA NUCLEARE

Preventivo per l'anno ***2004***

Codice	Esperimento	Gruppo
	OPERA	2
Resp. loc.: Giuseppe Grella		

Struttura
SA

COMPOSIZIONE DEL GRUPPO DI RICERCA

N	RICERCATORE Cognome e Nome	Qualifica				Affer. al gruppo	%
		Dipendenti		Incarichi			
		Ruolo	Art. 23	Ricerca	Assoc.		
1	Barbuto Emiliano				AsRic	2	100
2	Grella Giuseppe			P.O.		2	80
3	Romano Giorgio			P.O.		2	100
4	Sirignano Chiara				Dott.	2	100
	Numero totale dei ricercatori						4
	Ricercatori Full Time Equivalent						3.8

N	TECNOLOGI Cognome e Nome	Qualifica			%
		Dipendenti		Incarichi	
		Ruolo	Art. 23	Ass. Tecnol.	
1	Bozza Cristiano		Art.23		100
	Numero totale dei Tecnologi				1
	Tecnologi Full Time Equivalent				1

N	TECNICI Cognome e Nome	Qualifica				%
		Dipendenti		Incarichi		
		Ruolo	Art. 15	Collab. tecnica	Assoc. tecnica	
1	Di Marino Maurizio			Univ.		100
	Numero totale dei Tecnici					1
	Tecnici Full Time Equivalent					1

SERVIZI TECNICI

Denominazione	mesi−uomo

Annotazioni:

Osservazioni del direttore della struttura in merito alla disponibilità di personale e attrezzature

Mod EC./EN. 7 (a cura del responsabile locale)

ISTITUTO NAZIONALE DI FISICA NUCLEARE

Preventivo per l'anno ***2004***

Codice	Esperimento	Gruppo
	OPERA	2
Rapp. Naz.: Muciaccia Maria Teresa		

MILESTONES PROPOSTE PER IL 2004

Data completamento	Descrizione
31/12/2004	Fine montaggio primo magnete e mezza installazione secondo magnete
31/12/2004	Inizio installazione wall
31/12/2004	Realizzazione prototipo catena di sviluppo per lastre di emulsioni
31/12/2004	Fine produzione RPC e completamento installazione nel primo spettrometro
31/12/2004	Sviluppo e test per la strategia di localizzazione e misura di vertici di interazioni
31/12/2004	Installazione e tuning di almeno un microscopio finale in tutti i laboratori
31/12/2004	Realizzazione e prove di funzionamento in ditta della BAM

ISTITUTO NAZIONALE DI FISICA NUCLEARE
Preventivo per l'anno ***2004***

Struttura	Gruppo
SA	2
Coordinatore: Bruno Bartoli	

COMPOSIZIONE DEI GRUPPI DI RICERCA: A) − RICERCATORI

Componenti del Gruppo e ricerche alle quali partecipano:

N.	Cognome e Nome	Qualifica				Affer. al gruppo	Ricerche del gruppo in %										Percentuale impegno in altri gruppi				Altri impegni
		Dipendenti		Incarichi																	
		Ruolo	Art. 23	Ricerca	Assoc.		OPERA	MAGO									I	III	IV	V	
1	Barbuto Emiliano				AsRic	2	100														
2	Croce Rocco P.				AsRic	2		20													80
3	Galdi Vincenzo			P.A.		2		20													80
4	Grella Giuseppe			P.O.		2	80											20			
5	Pierro Vincenzo			P.A.		4		30											30		40
6	Pinto Innocenzo			P.O.		4		30											30		40
7	Romano Giorgio			P.O.		2	100														
8	Sirignano Chiara				Dott.	2	100														
						Ricercatori	3.8	1													

Note:

INSERIRE I NOMINATIVI IN ORDINE ALFABETICO **(N.B.NON VANNO INSERITI I LAUREANDI)**

1) PER I DIPENDENTI — Indicare il profilo INFN
2) PER GLI INCARICHI DI RICERCA — Indicare la Qualifica Universitaria (P.O. P.A. R.U.) o Ente di rappresentanza
3) PER GLI INCARICHI DI ASSOCIAZIONE — Indicare la Qualifica Universitaria o Ente di appartenenza per Dipendenti altri Enti: Bors.) Borsista; B−P−D) Post−Doc; B.Str.) Borsista straniero; Perf.) Perfezionando; Dott.) Dottorando; AsRic) Assegno di ricerca; S.Str) Studioso straniero; DIS) Docente Istituto Superiore
4) INDICARE IL GRUPPO DI AFFERENZA

(N.B.NON VANNO INSERITI I LAUREANDI)

Mod G1

Struttura	Gruppo
SA	2
Coordinatore: Bruno Bartoli	

ISTITUTO NAZIONALE DI FISICA NUCLEARE

Preventivo per l'anno ***2004***

COMPOSIZIONE DEI GRUPPI DI RICERCA: B) − TECNOLOGI

Componenti del Gruppo e ricerche alle quali partecipano:

N.	**Cognome e Nome**	**Qualifica**			**Ricerche del gruppo in %**										Percentuale impegno in altri gruppi				**Altri impegni**
		Dipendenti		Incarichi															
		Ruolo	Art. 23	Assoc. Tecnologica	OPERA										I	III	IV	V	
1	Bozza Cristiano		Art.23		100														

Note:

1) PER I DIPENDENTI — Indicare il profilo INFN
2) PER GLI INCARICHI DI ASSOCIAZIONE — Indicare Ente da cui dipendono, Bors. T.) Borsista Tecnologo

Mod G2

ISTITUTO NAZIONALE DI FISICA NUCLEARE	Struttura	Gruppo
Preventivo per l'anno ***2004***	SA	2
	Coordinatore: Bruno Bartoli	

COMPOSIZIONE DEI GRUPPI DI RICERCA: C) − TECNICI

Componenti del Gruppo e ricerche alle quali partecipano:

N.	Cognome e Nome	Qualifica				Ricerche del gruppo in %										Percentuale impegno in altri gruppi				Altri impegni
		Dipendenti		Incarichi																
		Ruolo	Art. 23	Collab. tecnica	Assoc. Tecnica	OPERA										I	III	IV	V	
1	Di Marino Maurizio			Univ.		100														
Servizi (mesi−uomo)																				
	−− Vuoto −−																			

Note:

1) PER I DIPENDENTI — Indicare il profilo INFN
2) PER GLI INCARICHI DI COLLABORAZIONE TECNICA — Indicare Ente da cui dipendono
3) PER GLI INCARICHI DI ASSOCIAZIONE TECNICA — Indicare Ente da cui dipendono

Mod G3

ISTITUTO NAZIONALE DI FISICA NUCLEARE
Preventivo per l'anno ***2004***

Struttura	Gruppo
SA	2
Coordinatore: Bruno Bartoli	

PREVISIONE DELLE SPESE DI DOTAZIONE E GENERALI DI GRUPPO

Dettaglio della previsione delle spese del Gruppo che non afferiscono
ai singoli esperimenti e per l'ampliamento della Dotazione di base del Gruppo

In KEuro

VOCI DI SPESA		DESCRIZIONE DELLA SPESA	IMPORTI Parziali	IMPORTI Totale Compet.
Viaggi e missioni	**Interno**	Congressi nazionali e contatti con altri laboratori.	4.0	**4.0**
Viaggi e missioni	**Estero**	Congressi internazionali e contatti con laboratori esteri.	8.0	**8.0**
Materiale di consumo		Materiale di consumo per strutture di calcolo di gruppo e varie.	4.0	**4.0**
Spese Seminari		Seminari.	1.0	**1.0**
Trasporti e facch.				**0.0**
Pubblicazioni Scientifiche		Pubblicazioni.	1.0	**1.0**
Spese Calcolo		Consorzio: ; Ore CPU: ; Spazio Disco: ; Cassette: ; Altro:		**0.0**
Affitti e Manutenzione Apparecchiature (1)				**0.0**
Materiale inventariabile		Supporto di apparecchiature di calcolo di gruppo.	5.0	**5.0**
			Totali	**23.0**

(1) Indicare tutte le macchine in manutenzione

Mod G4 (a cura del responsabile locale)

ISTITUTO NAZIONALE DI FISICA NUCLEARE
Preventivo per l'anno ***2004***

Struttura	Gruppo
SA	2

PREVISIONE DELLE SPESE PER LE RICERCHE

RIEPILOGO DELLE SPESE PREVISTE PER LE RICERCHE DEL GRUPPO

In KEuro

	SIGLA ESPERIMENTO	SPESA PROPOSTA										
		Miss. interno	Miss. estero	Mater. di cons.	Spese Semin.	Trasp e Facch.	Pubbl. Scient.	Spese Calc.	Aff. e Manut. App.	Mater. Invent.	Costruz. Appar.	TOT Compet.
A) Esperimenti o Iniz.Specifiche Gr.IV in Corso	OPERA	34.0	50.5	44.5		0.0		0.0	0.0	0.0	72.0	201.0
Totali A)		**34**	**50.5**	**44.5**	**0**	**0**	**0**	**0**	**0**	**0**	**72**	**201**
B) Esperimenti o Iniz.Specifiche Gr.IV da Iniziare	MAGO	15.0	20.0	0.0		0.0		0.0	10.0	20.0	0.0	65.0
Totali B)		**15**	**20**	**0**	**0**	**0**	**0**	**0**	**10**	**20**	**0**	**65**
C) Dotazioni di Gruppo		**4.0**	**8.0**	**4.0**	**1.0**	**0.0**	**1.0**	**0.0**	**0.0**	**5.0**	**0.0**	**23.0**
Totali (A+B+C)		**53**	**78.5**	**48.5**	**1**	**0**	**1**	**0**	**10**	**25**	**72**	**289**

Mod G5